

Microscopic nonsecular master equation for thermally open pseudo-Hermitian quantum systems

by

Felix Ivander

A thesis submitted in partial satisfaction of the

requirements for the degree of

Masters of Science

in

Chemistry

in the

Graduate Division

of the

University of California, Berkeley

Committee in charge:

Professor K. Birgitta Whaley, Chair

Professor David T. Limmer

Professor Ori J. Ganor

Summer 2023

Microscopic nonsecular master equation for thermally open pseudo-Hermitian quantum systems

Copyright 2023
by
Felix Ivander

Contents

Contents	i
1 Introduction	1
2 Pseudo-hermitian Redfield Master Equation	4
3 Applications A: Triangular Hamiltonian	12
4 Applications B: Two level gain-loss \mathcal{PT} -symmetric Hamiltonian	14
5 Applications C: Three-level gain-loss \mathcal{PT} -symmetric Hamiltonian	22
6 Discussion and Outlook	29
A Pseudo-hermitian master equations in the Lindblad form	31
B Generalized Non-hermitian Redfield Master Equation	34
C Applications D: Asymmetric σ_y -type Hamiltonian	35
Bibliography	38

Acknowledgments

I thank Prof. Birgitta Whaley for her guidance and mentoring, and Profs. David Limmer and Ori Ganor for careful reading of this thesis. We acknowledge fruitful discussions with Robert L. Cook, Philippe Lewalle, Zengzhao Li, and Liwen Ko; and useful inputs from Nicholas Anto-Sztrikacs, Kater W. Murch, Sahin Ozdemir, Weijian Chen, and Qi Zhong.

Chapter 1

Introduction

The hermiticity of a Hamiltonian is a sufficient—yet not necessary—condition for the reality of its energy eigenvalues [1, 2, 3]. Non-hermitian Hamiltonians (**NHs**) arise naturally as effective descriptions of dissipative systems from the classical (e.g., in acoustics [4], photonics [5, 6, 7], optical microcavities [8, 9], magnetic systems [10], and population biology [11]) to quantum (e.g., particle decay [12, 13], condensed matter systems [14], and superradiance [15], in addition to conventional open quantum systems) regimes [16]. NHs admit complex-valued eigenspectra, resulting to the emergence of exceptional points (**EPs**) in parameter space where multiple eigenmodes (i.e., both eigenvalues and eigenvectors) coalesce and bifurcate under sublinear scaling [17]. Beyond signifying phase transitions, nontrivial effects were theoretically predicted and furthermore realized in a wide variety of experimental platforms [18, 19, 20, 21, 22, 23, 24] in close proximity to EPs; enhanced sensing [25], dynamical acceleration [26, 27], accelerated generation of entanglement [28], induced chirality [20, 21], skin effect [29, 30, 31, 32, 33], unidirectional invisibility [34, 35], as examples of a rich literature [16]. It is a contemporary interest to understand and harness non-Hermitian phenomena for potential practical applications.

The *universal* strategy to study non-Hermitian quantum dynamics is through the GKSL (Gorini–Kossakowski–Sudarshan–Lindblad) master equation framework. Neglecting the quantum jump terms, e.g., experimentally via postselection, yields an effective non-Hermitian Hamiltonian exhibiting Hamiltonian Exceptional Points (**HEPs**) [28]. A more complete description of an open system retains this term, and are therefore concerned with Liouvillian Exceptional Points (**LEPs**). The latter has recently garnered tremendous research attention [27, 36, 23, 37, 26, 38]. Within both formalisms, *hermitian* quantum systems are embedded with effective non-Hermitian features, arising from a *Markovian* environment that is *weakly coupled*. To the best of our knowledge, apart from Refs. [39, 40, 41, 42] (which are generalizations of the **GKSL** equation, and therefore phenomenological), no other studies has addressed *intrinsically pseudo*-Hermitian systems interacting with a structured thermal environment.

Pseudo-hermitian Hamiltonians (**PHs**) are related to its hermitian conjugate via a similarity transform through a Hermitian and invertible metric η , $\hat{H}^\dagger = \eta \hat{H} \eta^{-1}$ [43, 44]. There-

fore, their eigenenergies are either all real or they come in complex conjugate pairs. This class of non-hermitian hamiltonians encompasses \mathcal{PT} -symmetric systems, where η is \mathcal{P} ; and hermitian hamiltonians, with η as the identity. Pseudo-Hermitian Hamiltonians satisfy a modified von-Neumann equation $\frac{\partial}{\partial t}(\rho\eta) = \frac{1}{i\hbar}[\dot{H}, \rho\eta]$, and a modified interaction picture $U(t)\rho\eta U^{-1}(t)$, in which frame one may perform the Born-Markov perturbative procedure. Significantly, a PHH open to a structured environment can be mapped to a hermitian system interacting with environments obeying the Born-Markov approximation *in addition* to a special environment which is treated properly without approximations, accounted by the pseudo-hermitian decay terms (hence opening the possibility to study strongly coupled non-Markovian interactions). This configuration encompasses a wide class of systems where the interplay of non-hermitian and thermal effects is relevant, including as a concrete example a nonhermitian transmon [37] immersed in thermal phononic or spin baths.

Master equations of the Redfield form in general do not recast to a GKSL form, and therefore they are not a completely positive and trace preserving (CPTP) map [45, 46, 47]. However, GKSL equation invokes the secular (rotating wave) approximation, which fails when the system's energy levels become near degenerate (occurring *precisely* around exceptional points). Furthermore, quantum coherent effects are more comprehensively incorporated through a nonsecular theory—what are the manifestations of nonsecular effects in the context of pseudo-hermitian quantum dynamics? A master equation of a Redfield form is an appealing option to address these questions, yet the very first steps of the usual microscopic derivation is rendered invalid once the Hamiltonian is not anymore Hermitian.

In this thesis we develop a nonsecular quantum master equation which deals *directly* with a pseudo-hermitian quantum system. This takes the microscopic Redfield form with a few important generalizations, e.g., in the broken phase, the environment spectral density admits complex Bohr frequencies. Our approach tackles non-Hermitian open quantum dynamics from a fresh angle, elucidating (1) the interplay of thermal and non-hermitian effects, and (2) the impacts of temperature to exceptional points, while treating the system fully microscopically. This formalism further addresses the thermalization behaviour of a pseudo-hermitian Hamiltonian [48, 49]. We apply the Pseudo-hermitian Redfield Equation (PHRE) to study central and overlooked problems in quantum dynamics. Namely, we study pseudo-hermitian effects in (1) a triangular hamiltonian, (2) gain-loss \mathcal{PT} -symmetric qubit hamiltonian [50], and (3) gain-loss quasi-degenerate three-level system. As there is currently no numerically exact method for this class of systems, we compare with the analogous generalized Lindblad equation (GLE) described in Ref. [40]. With the PHRE formalism, we highlight a number of key new results:

(1) Opening the pseudohermitian quantum system to a thermal environment displaces exceptional points in parameter space. These LEPs are typically of lower order than the corresponding LEPs as the system is closed.

(2) The extent of displacement of the LEPs depends on temperature, coupling strength, and structure of the thermal bath. Specifically, Ohmic baths display this behaviour while superohmic baths do not. Both dependence and selectivity offer promise of quantum sensing and information processing applications.

(3) We introduced a *generalized* spectral density of the thermal bath to include responses from imaginary Bohr frequencies. While arising from a mathematical motivation, this additional and unprobed degree of freedom can have interesting implications on both the dynamics and eigenspectrum of the pseudohermitian system.

(4) Prethermalization behaviour arise from nonhermitian gain-loss terms, manifesting in the three level \mathcal{PT} -symmetric Hamiltonian. Here, integrability breaking is induced by the gain-loss term instead of a small splitting, since excited states are fully degenerate.

(5) The steady-state of the normalized system density matrix of a pseudohermitian Hamiltonian can be highly nontrivial and distinct even qualitatively from the Gibbs state. For instance, for the three level \mathcal{PT} -symmetric Hamiltonian with otherwise identical parameters, simply varying temperature can modify whether the excited states (experiencing gain-loss) is more populated than the ground state or otherwise, at steady state.

(6) We push the limit of the PHRE method through investigating an example where unphysical results are predicted. PHRE suffers from the detriments of Redfield QME not being a CPTP map, with particular systems amplifying this problem. For a wide range of systems we study in the main thesis, we confirm numerically that these problems do not arise.

This thesis is organized as follows. In Ch. 2 we review the pseudo-hermitian formulation of quantum mechanics and derive the Pseudo-Hermitian Redfield Quantum Master equation. We apply this method to investigate archetypal pseudohermitian systems: a triangular Hamiltonian in Ch. 3, the two-level gain-loss \mathcal{PT} -symmetric Hamiltonian in Ch. 4, in Ch. 5 we discuss the three-level analog, and in Appendix C we discuss the asymmetric σ_y -type Hamiltonian. We discuss and conclude in Ch. 6. Appendix A concerns pseudo-hermitian master equations in Lindblad form and Appendix B discusses briefly the generalized non-hermitian Redfield Master Equation.

Chapter 2

Pseudo-hermitian Redfield Master Equation

Before we detail the derivation of the Pseudo-hermitian Redfield Master Equation, which builds on the bare Redfield equation, first we argue why the latter is not applicable to tackle systems relevant in this thesis. There are two main reasons:

1. In contrast to equations in the GKLS form, Redfield equation cannot nicely segregate the quantum jump and nonunitary coherent terms (see Appendix A). Such a separation is necessary to construct an effective nonhermitian Hamiltonian, and it requires making the secular approximation.
2. Incorporating spontaneous decay terms is critical to model nonhermitian systems. However, due to its constraints standard Redfield equation cannot model spontaneous decay (i.e., through having a special kind of decay bath). This is somewhat obvious from symmetry arguments (namely the system coupling operator must be of the form $\hat{S} \propto |i\rangle\langle i|$, one will find this yields no dynamics.). The decay terms can be added by hand in the equations of motion, but then the objective of this thesis is to study emergent effects from microscopic principles.

Now that some motivation have been laid out we start the derivation of PHRE. An η -pseudo-Hamiltonian \hat{H}_S satisfies

$$\hat{H}_S^\dagger = \eta \hat{H}_S \eta^{-1}, \quad (2.1)$$

where the metric η is both Hermitian and invertible. Particularly, η is of indefinite signature: If η is a positive definite hermitian metric then the eigenvalues must be real, and cannot be complex. To see this, one can calculate $\langle \psi | \eta H | \psi \rangle$ for an eigenstate and use the fact that $\langle v | \eta | v \rangle$ is nonzero. The density matrix of a pure state is given by $\rho = |\psi\rangle\langle\psi|$, and with the Schrödinger equation $i\hbar|\dot{\psi}\rangle = \hat{H}_S|\psi\rangle$ we obtain

$$\dot{\rho} = |\dot{\psi}\rangle\langle\psi| + |\psi\rangle\langle\dot{\psi}|$$

$$\begin{aligned}
&= \frac{1}{i\hbar} \hat{H}_S |\psi\rangle\langle\psi| - \frac{1}{i\hbar} |\psi\rangle\langle\psi| \underbrace{\eta \hat{H}_S \eta^{-1}}_{\hat{H}_S^\dagger} \\
&\Rightarrow \dot{\rho}\eta = \partial_t(\rho\eta) = \frac{1}{i\hbar} [\hat{H}_S, \rho\eta],
\end{aligned} \tag{2.2}$$

where the last line was obtained by multiplying with η on both sides. For small systems the metric η can typically be found through trial-and-error, but systematic ways to obtain η have been described in e.g., Refs. [51, 52]. In particular, for pseudo-Hermitian matrices with real eigenvalues diagonalized by the matrix D , the metric η is given by $(DD^\dagger)^{-1}$. Properties of PHHs have recently been investigated in the context of quantum thermodynamics [53], for example on the generalization of the Jarzynski equality [54].

Here, we couple this pseudo-Hermitian system to a bosonic bath. The full Hamiltonian takes the form $\hat{H} = \hat{H}_S + \hat{H}_B + \hat{V}$, with

$$\hat{H}_B = \sum_j \omega_j \hat{b}_j^\dagger \hat{b}_j. \tag{2.3}$$

Here, \hat{b}_j^\dagger (\hat{b}_j) is the creation (annihilation) bosonic operator of a mode j of frequency ω_j . The system-bath interaction Hamiltonian is given in a linear bipartite form (neglecting the constant quadratic term), with a system operator \hat{S} coupled to a bath operator \hat{B} ,

$$\hat{V} = \hat{S} \otimes \hat{B}; \quad \hat{B} = \sum_j \lambda_j (\hat{b}_j^\dagger + \hat{b}_j). \tag{2.4}$$

λ_j describes the system-bath coupling energy between mode j in the bath and the system. Starting from Eq. (2.2) with $\hat{H}_0 = \hat{H}_S + \hat{H}_B$, we define the time evolution operator as

$$\hat{U}_0 = e^{-\frac{i}{\hbar} \hat{H}_0 t}, \tag{2.5}$$

which satisfies

$$\hat{U}_0^\dagger \eta \hat{U}_0 = \eta, \tag{2.6}$$

where it is understood that $\eta = \eta_S \otimes I$. Thus,

$$\begin{aligned}
|\psi(t)\rangle\langle\psi(t)|\eta &= U(t)|\psi(0)\rangle\langle\psi(0)|U^\dagger(t)\eta \\
&= U(t)|\psi(0)\rangle\langle\psi(0)|\eta U^{-1}(t) \\
&= U(t)\rho\eta U^{-1}(t).
\end{aligned} \tag{2.7}$$

Notice that:

$$\frac{\partial(\hat{U}_0 \rho \eta \hat{U}_0^{-1})}{\partial t} = \frac{i}{\hbar} \hat{H}_0 \hat{U}_0 \rho \eta \hat{U}_0^{-1} + \hat{U}_0 \frac{\partial \rho \eta}{\partial t} \hat{U}_0^{-1} - \hat{U}_0 \rho \eta \hat{U}_0^{-1} \frac{i}{\hbar} \hat{H}_0$$

$$= \hat{U}_0 \frac{\partial \rho\eta}{\partial t} \hat{U}_0^{-1} + [\hat{H}_0, (\rho\eta)_I] \quad (2.8)$$

where the subscript I indicates interaction representation, and that

$$\begin{aligned} \hat{U}_0[\hat{H}, \rho\eta]\hat{U}_0^{-1} &= \hat{U}_0[\hat{H}_0, \rho\eta]\hat{U}_0^{-1} + \hat{U}_0[\hat{V}, \rho\eta]\hat{U}_0^{-1} \\ &= [\hat{H}_0, (\rho\eta)_I] + [\hat{V}_I, (\rho\eta)_I]. \end{aligned} \quad (2.9)$$

So, subtracting Eq. (2.8) by Eq. (2.9),

$$\frac{\partial(\rho\eta)_I}{\partial t} = -\frac{i}{\hbar}[\hat{V}_I, (\rho\eta)_I]. \quad (2.10)$$

The formal solution to the above is given by (from now on $\rho\eta \rightarrow \tilde{\rho}$, and $\hbar \equiv 1$)

$$\tilde{\rho}_I(t) = \tilde{\rho}_I(t_0) - i \int_{t_0}^t [\hat{V}_I(\tau), \tilde{\rho}_I(\tau)] d\tau \quad (2.11)$$

To second order in the Dyson expansion

$$\frac{\partial \tilde{\rho}_I}{\partial t}(t) = -i[\hat{V}_I(t), \tilde{\rho}_I(t_0)] - \int_{t_0}^t d\tau [\hat{V}_I(t), [\hat{V}_I(\tau), \tilde{\rho}_I(\tau)]]. \quad (2.12)$$

At this point we follow standard Born-Markov derivation available in e.g., Refs. [47, 45, 46] only that $\sigma \rightarrow \tilde{\sigma}$ (note $\sigma \equiv \text{Tr}_B \rho$). Particularly, we make the weak coupling approximation $\tilde{\rho}(t) = \underbrace{\rho_S(t)\eta}_{\tilde{\sigma}(t)} \otimes \rho_B$ for all times (i.e., automatically assuming factorized initial condition),

assume the bath is static, and take the partial trace over the bath of the above. This yields

$$\frac{\partial \tilde{\sigma}_I}{\partial t}(t) = -i \text{Tr}_B \{ [\hat{V}_I(t), \tilde{\rho}_I(t_0)] \} - \text{Tr}_B \{ \int_{t_0}^t d\tau [\hat{V}_I(t), [\hat{V}_I(\tau), \tilde{\rho}_I(\tau)]] \} \quad (2.13)$$

The first term can be shown to vanish if $\text{Tr}[\hat{B}\rho_B(0)] = 0$ (automatically true for displacement operators which is an average of linear values). Further approximations are enumerated as follows: first Markov (fast bath) gives

$$\frac{\partial \tilde{\sigma}_I(t)}{\partial t} = -\text{Tr}_B \{ \int_{t_0}^t d\tau [\hat{V}_I(t), [\hat{V}_I(\tau), \tilde{\sigma}_I(t) \otimes \rho_B]] \}, \quad (2.14)$$

and second Markov:

$$\frac{\partial \tilde{\sigma}_I(t)}{\partial t} = -\text{Tr}_B \{ \int_0^\infty d\tau [\hat{V}_I(t), [\hat{V}_I(t-\tau), \tilde{\sigma}_I(t) \otimes \rho_B]] \}. \quad (2.15)$$

Approximations conclude. Recall that

$$\tilde{\sigma}_I(t) = e^{i\hat{H}_s t} \sigma(t) \eta e^{-i\hat{H}_s t}, \quad (2.16)$$

so the time derivative is

$$\frac{\partial \tilde{\sigma}_I}{\partial t}(t) = e^{i\hat{H}_s t} \frac{\partial \sigma \eta}{\partial t} e^{-i\hat{H}_s t} + \frac{i}{\hbar} [\hat{H}_s, (\sigma \eta)_I]. \quad (2.17)$$

With

$$e^{i\hat{H}_s t} \frac{\partial \sigma \eta}{\partial t} e^{-i\hat{H}_s t} = -\frac{i}{\hbar} [\hat{H}_s, (\sigma \eta)_I] - \text{Tr}_B \left\{ \int_0^\infty d\tau [\hat{V}_I(t), [\hat{V}_I(t-\tau), \tilde{\sigma}_I(t) \otimes \rho_B]] \right\}, \quad (2.18)$$

we rotate back to

$$\begin{aligned} \frac{\partial \sigma \eta}{\partial t} &= -\frac{i}{\hbar} e^{-i\hat{H}_s t} [\hat{H}_s, (\sigma \eta)_I] e^{i\hat{H}_s t} - \text{Tr}_B \left\{ \int_0^\infty d\tau e^{-i\hat{H}_s t} [\hat{V}_I(t), [\hat{V}_I(t-\tau), \tilde{\sigma}_I(t) \otimes \rho_B]] e^{i\hat{H}_s t} \right\} \\ &= -\frac{i}{\hbar} [\hat{H}_s, \sigma \eta] - \text{Tr}_B \left\{ \int_0^\infty d\tau e^{-i\hat{H}_s t} [\hat{V}_I(t), [\hat{V}_I(t-\tau), \tilde{\sigma}_I(t) \otimes \rho_B]] e^{i\hat{H}_s t} \right\} \end{aligned} \quad (2.19)$$

Our present objective is to simplify the integral, and we start by organizing the integrand

$$[\hat{V}_I(t), [\hat{V}_I(t-\tau), \tilde{\sigma}_I(t) \otimes \rho_B]] = [\hat{S}_I(t) \hat{B}_I(t), [\hat{S}_I(t-\tau) \hat{B}_I(t-\tau), \tilde{\sigma}_I(t) \rho_B]] \quad (2.20)$$

where \otimes have been suppressed. This expands to four terms

$$\hat{S}_I(t) \hat{S}_I(t-\tau) \tilde{\sigma}_I(t) \hat{B}_I(t) \hat{B}_I(t-\tau) \rho_B \quad (2.21)$$

$$- \hat{S}_I(t) \tilde{\sigma}_I \hat{S}_I(t-\tau)(t) \hat{B}_I(t) \rho_B \hat{B}_I(t-\tau) \quad (2.22)$$

$$- \hat{S}_I(t-\tau) \tilde{\sigma}_I(t) \hat{S}_I(t) \hat{B}_I(t-\tau) \rho_B \hat{B}_I(t) \quad (2.23)$$

$$+ \tilde{\sigma}_I(t) \hat{S}_I(t) \hat{S}_I(t-\tau) \rho_B \hat{B}_I(t-\tau) \hat{B}_I(t). \quad (2.24)$$

We take the partial trace, recall $\langle \rho \hat{A} \rangle = \text{Tr}\{\rho A\}$ and use cyclicity of trace, and also we multiply by $e^{-i\hat{H}_s t}$ and $e^{i\hat{H}_s t}$ on both sides to get

$$\hat{S} e^{-i\hat{H}_s \tau} \hat{S} e^{i\hat{H}_s \tau} \tilde{\sigma}(t) \langle \hat{B}_I(t) \hat{B}_I(t-\tau) \rangle \quad (2.25)$$

$$- \hat{S} \tilde{\sigma}(t) e^{-i\hat{H}_s \tau} \hat{S} e^{i\hat{H}_s \tau} \langle \hat{B}_I(t-\tau) \hat{B}_I(t) \rangle \quad (2.26)$$

$$- e^{-i\hat{H}_s \tau} \hat{S} e^{i\hat{H}_s \tau} \tilde{\sigma}(t) \hat{S} \langle \hat{B}_I(t) \hat{B}_I(t-\tau) \rangle \quad (2.27)$$

$$+ \tilde{\sigma}(t) e^{-i\hat{H}_s \tau} \hat{S} e^{i\hat{H}_s \tau} \hat{S} \langle \hat{B}_I(t-\tau) \hat{B}_I(t) \rangle. \quad (2.28)$$

Organizing these terms as a commutator gives

$$[\hat{S}, e^{-i\hat{H}_s \tau} \hat{S} e^{i\hat{H}_s \tau} \tilde{\sigma}(t)] \langle \hat{B}_I(t-\tau) \hat{B}_I(t) \rangle - [\hat{S}, \tilde{\sigma}(t) e^{-i\hat{H}_s \tau} \hat{S} e^{i\hat{H}_s \tau}] \langle \hat{B}_I(t) \hat{B}_I(t-\tau) \rangle, \quad (2.29)$$

and thus the master equation reduces to

$$\frac{\partial \sigma \eta}{\partial t} = -\frac{i}{\hbar} [\hat{H}_s, \sigma \eta] - \int_0^\infty \left\{ [\hat{S}, e^{-i\hat{H}_s \tau} \hat{S} e^{i\hat{H}_s \tau} \sigma(t) \eta] \langle \hat{B}_I(t-\tau) \hat{B}_I(t) \rangle \right.$$

$$-[\hat{S}, \sigma(t)\eta e^{-i\hat{H}_s\tau}\hat{S}e^{i\hat{H}_s\tau}]\langle\hat{B}_I(t)\hat{B}_I(t-\tau)\rangle\Big\} d\tau. \quad (2.30)$$

Recall \hat{H}_s can, in general, have complex eigenvalues. Specifically, pseudo-Hermitian matrices have eigenvalues that are real or come in complex conjugate pairs [52].

Assuming a stationary bath $\langle\hat{B}_I(t)\hat{B}_I(t-\tau)\rangle = \langle\hat{B}_I(\tau)\hat{B}_I(0)\rangle$, and since in the energy basis of \hat{H}_s , $[\hat{H}_s, \sigma\eta]_{ab} = (E_a - E_b)(\sigma\eta)_{ab}$, one recovers a Redfield-type master equation

$$\begin{aligned} \dot{\tilde{\sigma}}_{ab}(t) &= -i\omega_{ab}\tilde{\sigma}_{ab}(t) \\ &- \sum_{c,d,m} \left\{ R_{ac,cd}^m(\omega_{dc})\tilde{\sigma}_{db}(t) + R_{bd,dc}^{m,*}(\omega_{cd})\tilde{\sigma}_{ac}(t) \right. \\ &\left. - [R_{db,ac}^m(\omega_{ca}) + R_{ca,bd}^{m,*}(\omega_{db})]\tilde{\sigma}_{cd}(t) \right\}. \end{aligned} \quad (2.31)$$

If the Bohr frequencies are entirely real, the Redfield tensor can be evaluated via standard procedures [47],

$$\begin{aligned} R_{ij,kl}(\omega) &= S_{ij}S_{kl} \int_0^\infty d\tau e^{i\omega\tau} \langle\hat{B}_I(\tau)\hat{B}_I(0)\rangle \\ &= S_{ij}S_{kl} \int_0^\infty d\tau e^{i\omega\tau} \sum_j \lambda_j^2 [e^{i\omega_j t} \langle\hat{n}(\omega_j)\rangle + e^{-i\omega_j t} \langle\hat{n}(\omega_j) + 1\rangle], \end{aligned} \quad (2.32)$$

where $S_{ij} \equiv \langle i|\hat{S}|j\rangle$. This expression is obtained by evaluating the bath correlation function,

$$\begin{aligned} \langle\hat{B}_I(\tau)\hat{B}_I\rangle &= \left\langle \sum_j \lambda_j (\hat{b}_j^\dagger e^{i\omega_j t} + \hat{b}_j e^{-i\omega_j t}) \sum_k \lambda_k (\hat{b}_k^\dagger + \hat{b}_k) \right\rangle \\ &= \sum_{j,k} \lambda_j \lambda_k [\langle\hat{b}_j^\dagger e^{i\omega_j t} \hat{b}_k^\dagger\rangle + \langle\hat{b}_j^\dagger e^{i\omega_j t} \hat{b}_k\rangle + \langle\hat{b}_j e^{-i\omega_j t} \hat{b}_k^\dagger\rangle + \langle\hat{b}_j e^{-i\omega_j t} \hat{b}_k\rangle] \\ &= \sum_j \lambda_j^2 [\langle\hat{b}_j^\dagger e^{i\omega_j t} \hat{b}_j\rangle + \langle\hat{b}_j e^{-i\omega_j t} \hat{b}_j^\dagger\rangle] \\ &= \sum_j \lambda_j^2 [e^{i\omega_j t} \langle\hat{n}(\omega_j)\rangle + e^{-i\omega_j t} \langle\hat{n}(\omega_j) + 1\rangle] \end{aligned} \quad (2.33)$$

The third equality is due to (1) the assumption that the bath is composed of uncorrelated harmonic modes (i.e. operators acting on different modes commute) so the summation is non-zero only when $j = k$, and (2) the terms $\langle\hat{b}_j^\dagger e^{i\omega_j t} \hat{b}_j^\dagger\rangle$ and $\langle\hat{b}_j e^{-i\omega_j t} \hat{b}_j\rangle$ vanish in matrix form as e.g., $\hat{b}_j e^{-i\omega_j t} \hat{b}_j$ is non-diagonal. The expectation value of the number operator of mode j , $\langle\hat{n}(\omega_j)\rangle$, is assumed to take the Bosé-Einstein distribution form, $n_B(\omega) \equiv \frac{1}{e^{\beta\omega} - 1}$. We add a vanishing imaginary frequency $\omega \rightarrow \omega + i\epsilon$ and use the Sokhotski-Plemelj theorem,

$$\lim_{\epsilon \rightarrow 0^+} \frac{1}{x \pm i\epsilon} = \mp i\pi\delta(x) + \mathcal{P}\left(\frac{1}{x}\right), \quad (2.34)$$

which yields

$$\text{Re} \left\{ \int_0^\infty d\tau e^{i\omega\tau} \langle \hat{B}_I(\tau) \hat{B}_I(0) \rangle \right\} = \begin{cases} \pi J(\omega) n(|\omega|) & \omega < 0 \\ \pi J(\omega)[(n(\omega) + 1)] & \omega > 0 \\ \pi \lim_{\omega \rightarrow 0^+} J(\omega) n(|\omega|) & \omega = 0, \end{cases} \quad (2.35)$$

with the spectral density $J(\omega) = \sum_k \lambda_k^2 \delta(\omega - \omega_k)$. For an ohmic bath with slope γ , it was shown in e.g., Ref. [55] that $\lim_{\omega \rightarrow 0^+} J(\omega) n(|\omega|) = \frac{\gamma}{\beta}$. The imaginary part of the Laplace transform,

$$\text{Im} \left\{ \int_0^\infty d\tau e^{i\omega\tau} \langle \hat{B}_I(\tau) \hat{B}_I(0) \rangle \right\} \equiv Z(\omega) = \frac{1}{\pi} \mathcal{P} \int_{-\infty}^\infty d\omega' \frac{\Gamma(\omega')}{\omega - \omega'}, \quad (2.36)$$

where \mathcal{P} denotes principal value of the integral, will need to be computed explicitly via e.g., Matsubara frequency summation [56, 57]. For numerical simulations in the main paper, this contribution is neglected as it is vanishing at high enough temperatures for Ohmic spectral densities, as was shown in Ref. [56]. If the Bohr frequencies admit complex values, $\omega = \omega_R + i\omega_I$, even in the diagonal basis the Hamiltonian is nonhermitian. In the pseudo-interaction picture, the creation (annihilation) operator is still $b_k^\dagger e^{i\omega t}$ ($\hat{b}_k e^{-i\omega t}$) and

$$R_{ij,kl}(\omega_R + i\omega_I) = S_{ij} S_{kl} \int_0^\infty d\tau e^{-\omega_I\tau} \sum_j \lambda_j^2 [e^{i(\omega_R + \omega_j)\tau} n_B(\omega_j) + e^{i(\omega_R - \omega_j)\tau} (n_B(\omega_j) + 1)]. \quad (2.37)$$

The integral converges always when $\omega_I > 0$, in which case

$$\int_0^\infty \lambda_j^2 n_B(\omega_j) e^{-\omega_I\tau} e^{i(\omega_R + \omega_j)\tau} d\tau = \frac{\lambda_j^2 n_B(\omega_j)}{\omega_I + i(\omega_R + \omega_j)}, \quad (2.38)$$

and

$$\int_0^\infty \lambda_j^2 (n_B(\omega_j) + 1) e^{-\omega_I\tau} e^{i(\omega_R - \omega_j)\tau} d\tau = \frac{\lambda_j^2 (n_B(\omega_j) + 1)}{\omega_I + i(\omega_R - \omega_j)}, \quad (2.39)$$

which will have no poles unless ω_j is complex. Therefore, here we introduce a **hand-wavy** workaround which is essentially a quick fix ansatz. More physical justification will be delegated to a future work.

We let the bath modes possess finite imaginary frequencies, $\omega_J = \omega_{J,R} + i\omega_{J,I}$, and assuming $J^G(\omega_R, \omega_I) = J_R(\omega_R) J_I(\omega_I) = \sum_j \lambda_{j,R}^2 \delta(\omega_R - \omega_{j,R}) \sum_k \lambda_{k,I}^2 \delta(\omega_I - \omega_{k,I})$, this recovers Eq. (2.35) only that $J(\omega) \rightarrow J^G(\omega_R, \omega_I)$. If $\omega_I < 0$, a different regularization procedure is needed to evaluate the Laplace transform, following [58], through introducing a small real parameter x ,

$$G(\omega, \epsilon) = \int_0^\infty dx e^{-\epsilon x^2} e^{i\omega x} = \frac{i}{\omega} \sqrt{\pi} w e^{w^2} \text{erfc}(w) \quad (2.40)$$

where $w = -i\omega/(2\sqrt{\epsilon})$. $G(\omega, \epsilon \rightarrow 0^+)$ converges to $\frac{i}{\omega}$ provided $-\frac{\pi}{4} < \arg \omega < \frac{5}{4}\pi$, and this is assumed in this thesis. Otherwise, the integral converges given sufficiently behaving λ_I , which is assured given appropriate imaginary spectral density (e.g., decaying sufficiently fast in both real and imaginary parts). Recollecting our results,

$$\text{Re} \left\{ \int_0^\infty d\tau e^{i(\omega_R + i\omega_I)\tau} \langle \hat{B}_I(\tau) \hat{B}_I(0) \rangle \right\} = \begin{cases} \pi J^G(\omega_R, \omega_I) n(|\omega_R|) & \omega_R < 0 \\ \pi J^G(\omega_R, \omega_I)[(n(\omega_R) + 1) & \omega_R > 0. \\ \pi \lim_{\omega \rightarrow 0^+} J(\omega) n(|\omega|) & \omega_R = 0, \end{cases} \quad (2.41)$$

and we still demand the Bosé-Einstein distribution function to be insensitive to ω_I . Essentially, the form of $J^G(\omega_R, \omega_I)$ is a degree of freedom of the environment. To follow we take $J^G(\omega_R, \omega_I) = J(\omega_R)$, although a damped spectral density $J^G(\omega_R, \omega_I) = J(\omega_R) e^{-\zeta \omega_I} e^{-\frac{\omega_I}{\omega_{c,I}}}$ can also be chosen.

It is natural to think about the extension proposed here on bath frequencies having finite imaginary components in terms of classical driven or damped harmonic oscillators. Namely, the bosonic thermal bath has now been generalized to contain driven and damped, on top of simple harmonic oscillators. Indeed, a few studies have reported the emergent need for this generalization especially when considering dissipative and open quantum systems [59, 60]. However, it is not trivial to quantize damped and driven classical oscillators, then consider a thermodynamic quantity of them, and finally proceeding in analogous fashion to retrieve the so-called generalized spectral density more rigorously. This problem is still yet unsolved and the literature on it is still very much an active area of research [61, 62].

In sum, the key step of deriving PHRE is the identification of a proper interaction picture if we evolve a *pseudo* density matrix $\rho\eta$, Eq. (2.10). This allows writing the master equation Eq. (2.30) which takes the familiar Redfield form, but (1) the system Hamiltonian \hat{H}_S can in principle admit complex eigenvalues, and (2) the differential equation involves a *pseudo* density matrix $\tilde{\sigma} \equiv \sigma\eta$. The *pseudo* density matrix, even though evolved as if it is a proper density matrix, is not required to satisfy basic properties: normalization, positivity, and purity conditions. The operation of the metric η could be thought of as a weak projector, so that when we rotate back to σ , a normalization procedure is taken,

$$\sigma(t) = \frac{\tilde{\sigma}(t)\eta^{-1}}{\text{Tr}\{\tilde{\sigma}(t)\eta^{-1}\}}. \quad (2.42)$$

Numerically, this procedure is done each timestep. However, one can add a nonlinear counterterm to ensure trace normalization [63].

Since the system Hamiltonian \hat{H}_S may admit complex eigenvalues, when evaluating the Laplace transform of the bath correlation function,

$$\begin{aligned} \int_0^\infty d\tau e^{-\omega_I \tau} \sum_j \lambda_j^2 & [e^{i(\omega_R + \omega_j)\tau} n_B(\omega_j) \\ & + e^{i(\omega_R - \omega_j)\tau} (n_B(\omega_j) + 1)], \end{aligned} \quad (2.43)$$

we find a new term $e^{-\omega_I \tau}$ probing a new dimension of the bath. Namely, assuming the transform converges, one finds that the spectral density of the bath must be generalized to include imaginary frequencies.

Throughout our analysis (except at the EP), left ($\langle L_i |$) and right ($| R_i \rangle$) eigenvectors, satisfying

$$\langle L_i | \hat{H} = E_i \langle L_i |, \quad \hat{H} | R_i \rangle = E_i | R_i \rangle \quad (2.44)$$

are biorthonormalized to satisfy relations in Refs. [64, 65]. Namely,

$$\langle L_i | R_j \rangle = \langle R_i^* | R_j \rangle \equiv \delta_{ij}, \quad (2.45)$$

while in general $\langle R_i | R_j \rangle \neq \delta_{ij}$.

Chapter 3

Applications A: Triangular Hamiltonian

We employ the formalism described in Ch. 2 to investigate a triangular Hamiltonian [66] Eq. (3.1), realized classically through nonreciprocal or unidirectional coupling between two energy levels, see e.g., Refs. [67, 68]. This Hamiltonian does not have decay terms yet it is still pseudo-hermitian, and therefore it is an example of a nonhermitian system that cannot result from an effective Lindblad description through neglecting quantum jumps. This triangular Hamiltonian system (THS),

$$\hat{H}_S^\Delta = \begin{bmatrix} \alpha & \gamma \\ 0 & \beta \end{bmatrix} = V \begin{bmatrix} \alpha & 0 \\ 0 & \beta \end{bmatrix} V^{-1}, \quad \alpha, \beta, \gamma \in \mathbb{R} \quad (3.1)$$

satisfies Eq. (2.1), where V is composed of eigenvectors $\begin{bmatrix} 1 \\ 0 \end{bmatrix}$, $\begin{bmatrix} -\frac{\gamma}{\alpha-\beta} \\ 1 \end{bmatrix}$, and

$$\eta = \begin{bmatrix} a & \frac{\gamma}{\alpha-\beta}a \\ \frac{\gamma}{\alpha-\beta}a & d \end{bmatrix}, \quad (3.2)$$

for some arbitrary numbers a and d . THS clearly has real eigenvalues. This is a good model to compare with nondissipative dynamics (i.e., $|\psi(t)\rangle = e^{-i\hat{H}_S^\Delta t}|\psi(0)\rangle$), which is simple enough to solve exactly. For instance, if we prepare the initial state $\rho(0) = x|g\rangle\langle g| + (1-x)|e\rangle\langle e|$, then at later times

$$\begin{aligned} \rho(t) &= e^{-i\hat{H}_S^\Delta t} \rho(0) e^{i(\hat{H}_S^\Delta)^\dagger t} \\ &= \begin{bmatrix} \frac{2(1-x)\gamma^2(\cos(\alpha-\beta)t-1)}{(\alpha-\beta)^2} + x & \frac{(1-e^{i(b-a)t})(x-1)\gamma}{\alpha-\beta} \\ \frac{(1-e^{-i(b-a)t})(x-1)\gamma}{\alpha-\beta} & 1-x \end{bmatrix}. \end{aligned} \quad (3.3)$$

The evolution of the density matrix is already not trace-preserving for nondissipative dynamics, i.e., $\text{Tr}\{\rho(t)\} = 1 + \frac{2(1-x)\gamma^2(\cos(\alpha-\beta)t-1)}{(\alpha-\beta)^2}$ as long as $\gamma \neq 0$. However, the density

matrix is still hermitian, with the coherences related by complex conjugates of each other. We now discuss opening this system to a thermal environment via $\hat{S} = \hat{\sigma}_x$ with the formalism described in Ch. 2. Simulation results are presented in Fig. (3.1), with a few important observations highlighted as follows: (1) One expects that the thermal state of the THS to mimic the case when $g = 0$, since its eigenvalues are dictated only by the diagonals, α and β . This is observed for the populations (after normalization) shown in panel (a). However, the THS develops coherences that become nonvanishing at steady-state, as seen in panel (b). This is characteristic of a Hamiltonian of the type $\frac{\Delta}{2}\sigma_z + \gamma\sigma_x$, and thus the thermally open THS behaves in between these two limits. (2) The coherences of the THS can at transient times not be complex conjugates of each other, and therefore in this sense the density matrix becomes nonhermitian. However, this is hardly surprising as the system unitary dynamics is dictated by a nonhermitian hamiltonian.

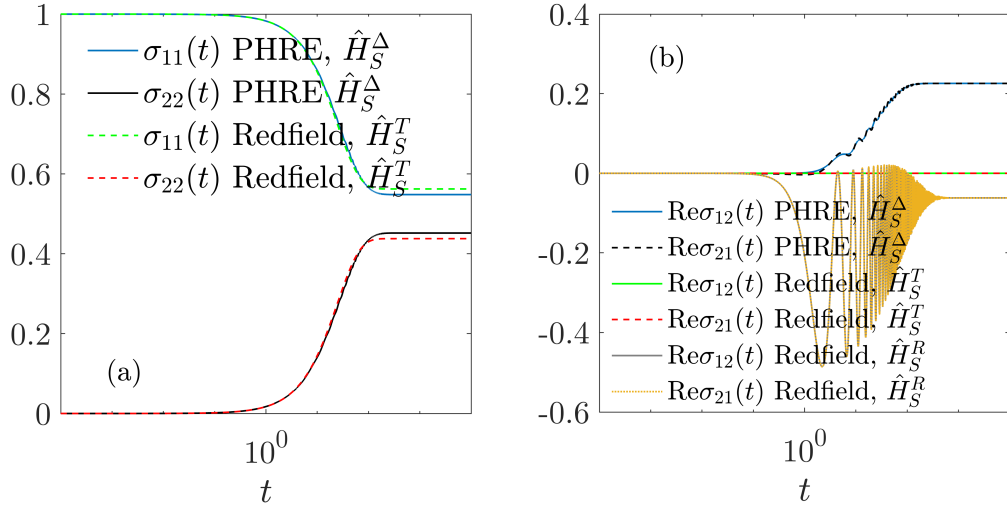


Figure 3.1: Simulations results using PHRE and standard Redfield. In panel (a), we plot the populations of \hat{H}_S^Δ , Eq. (3.1) using PHRE and $\hat{H}_S^T \equiv a|g\rangle\langle g| + b|e\rangle\langle e|$ using Redfield. In panel (b) we plot the real part of the coherences of \hat{H}_S^Δ , Eq. (3.1) using PHRE, and \hat{H}_S^T and $\hat{H}_S^R \equiv a|g\rangle\langle g| + b|e\rangle\langle e| + \gamma|g\rangle\langle e| + h.c.$, using Redfield. Parameters used are $a = 1$, $b = 2$, $\gamma = 0.5$, $T = 4$, and the bath spectral density is a Ohmic with slope 0.005 with an infinite energy cutoff.

Chapter 4

Applications B: Two level gain-loss \mathcal{PT} -symmetric Hamiltonian

One of the most archetypal model in the nonhermitian physics literature is the \mathcal{PT} -symmetric gain-loss Hamiltonian [69], Eq. (4.1),

$$\hat{H}_S = \begin{bmatrix} a - ib & g \\ g & a + ib \end{bmatrix}. \quad (4.1)$$

This system has been studied experimentally in various classical and quantum platforms, e.g. Ref. [18, 70, 71, 72, 73, 74], as it is a minimal model which displays robust nonhermitian properties. Yet even theoretically, studies (e.g., Refs. [36, 50]) investigating this model treated it without opening to a structured thermal environment through a phenomenological Lindblad description. Therefore they miss insight on the effects of microscopic properties e.g., having a phononic bath at a specific temperature or structure, to the robustness of exceptional points and deformation of the eigenspectrum. With eigenvalues $\lambda_{1,2} = a \mp \sqrt{g^2 - b^2}$ and eigenvectors $[-\frac{ib \pm \sqrt{g^2 - b^2}}{g}, 1]^T$, the Hamiltonian Eq. (4.1) has an exceptional point at $g = b$. When $g > b$ the eigenvalues are real and the system is in the so-called \mathcal{PT} -unbroken phase. When $g < b$, the eigenvalues are purely imaginary, and the system is in the \mathcal{PT} -broken phase.

Dynamics

PHRE has no problem simulating this model with metric $\eta = \hat{\sigma}_x$, but we first discuss dynamics of the system without coupling to a thermal bath as follows: the opposing limits of Eq. (4.1) are (1) when $b = 0$ where the system undergoes a Rabi-type oscillatory dynamics, which is well understood, and (2) when $g = 0$, where the model becomes a pure gain-loss Hamiltonian. With the initial state $\rho(0) = x|g\rangle\langle g| + (1-x)|e\rangle\langle e|$, the dynamics of the latter limit $g = 0$ satisfies

$$\rho(t) = \begin{bmatrix} e^{-2bt}x & 0 \\ 0 & (1-x)e^{2bt} \end{bmatrix}. \quad (4.2)$$

This analysis shows transparently the impacts of the non-hermitian terms $\pm ib$: the ground state decays to zero, while the excited state gains population indefinitely. The trace as a function of time is given by $\text{Tr}\{\rho(t)\} = \cosh 2bt + (1 - 2x) \sinh 2bt$, which is not unity in general.

In between these two limits, the impact of a nonvanishing g is to connect these two levels—one channel decay and another gain. This model is still simple enough to solve analytically,

$$\langle 1|\rho(t)|1\rangle = \frac{2bx\sqrt{g^2 - b^2} \sin(2t\sqrt{g^2 - b^2}) + (2b^2x + g^2(1 - 2x)) \cos(2t\sqrt{g^2 - b^2}) - g^2}{2(b^2 - g^2)}, \quad (4.3)$$

$$\langle 2|\rho(t)|2\rangle = \frac{g^2x \sin^2(t\sqrt{g^2 - b^2}) - (x - 1) \left(b \sin(t\sqrt{g^2 - b^2}) + \sqrt{g^2 - b^2} \cos(t\sqrt{g^2 - b^2}) \right)^2}{g^2 - b^2}, \quad (4.4)$$

$$\langle 1|\rho(t)|2\rangle = (\langle 2|\rho(t)|1\rangle)^* = \frac{ig \left((2x - 1)\sqrt{g^2 - b^2} \sin(2t\sqrt{g^2 - b^2}) + b \cos(2t\sqrt{g^2 - b^2}) - b \right)}{2(g^2 - b^2)}. \quad (4.5)$$

We now open this quantum system to a thermal environment via a $\hat{\sigma}_x$ -type interaction, simulated with PHRE (panels (a) and (b)) and Generalized Local Lindblad Equation [40] (GLE, panels (c) and (d), for details on this method see Appendix A) in Fig. (4.1). Note that for comparison, the rates in GLE were obtained via microscopic arguments used in PHRE. There are two regions of interest, shown in each panel pairs. Since both methods agree quantitatively in these two regimes, henceforth we discuss only the PHRE results. In panel (a) we simulate the \mathcal{PT} -symmetry broken phase. Here, the oscillatory behaviour driven by g is minimal and the system approaches equilibrium as dictated by an interplay of thermal and nonhermitian channels. However, as we defined the complex spectral density as $J^G(\omega_R, \omega_I) = J(\omega_R)$ (the imaginary part set constant) and since the Bosé-Einstein distribution only depends on ω_R , here the thermally-driven rate of excitation precisely equals the relaxation rate. In this case, thermal effects simply couple the two levels the same way g does without affecting steady-state populations. In panel (b), we consider the opposite limit, when $g \gg b$ and the system is in the unbroken phase. The dynamics in this regime is markedly different, with oscillatory behaviour taking over. Without the b term, the steady state would be an equal population of ground and excited states, yet here there is a finite population difference due to nonhermitian gain-loss asymmetry. Note, the fact that the system goes to a steady state at all in this regime is due to thermal effects.

Close to the Hamiltonian exceptional point $g = b$ both methods PHRE and GLE predict similar dynamics, as we discuss further in Appendix A. There is nothing special about the dynamics close to the Hamiltonian exceptional point for this model.

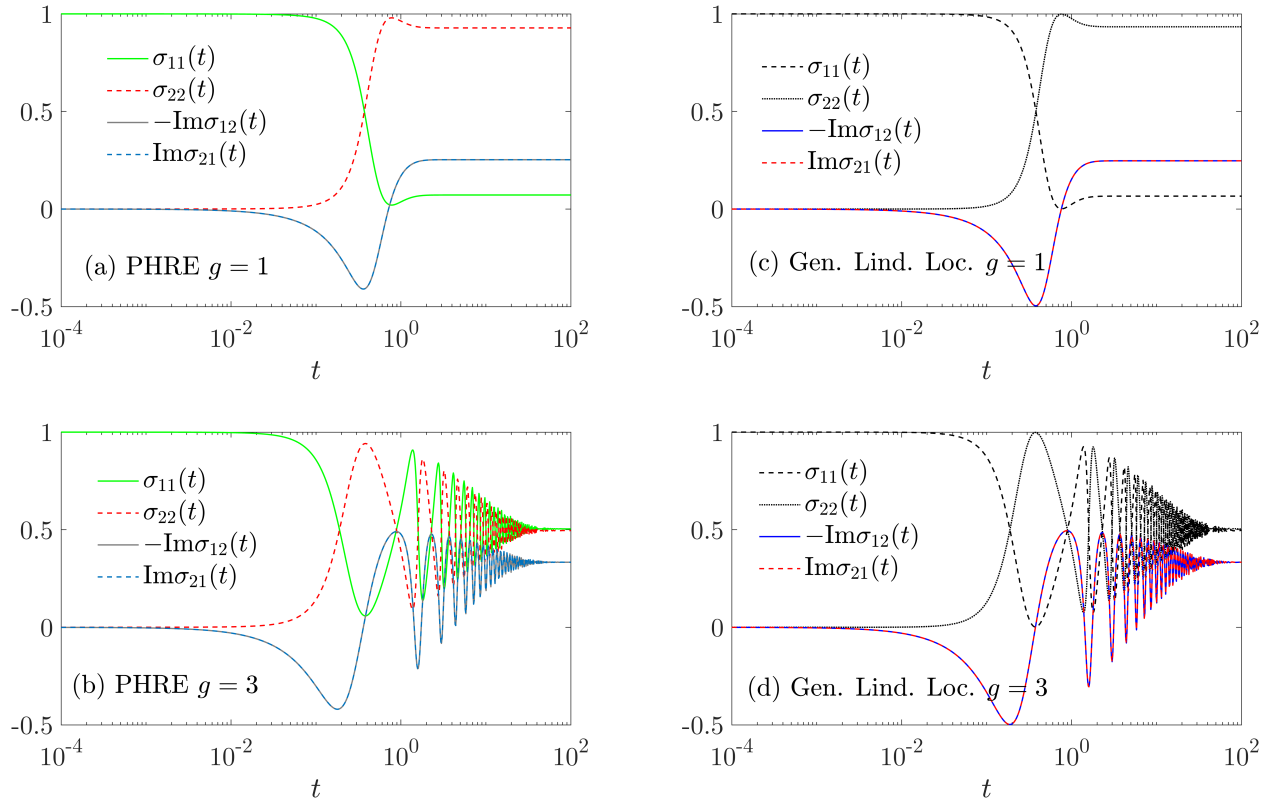


Figure 4.1: Simulations of density matrix evolution of the \mathcal{PT} -symmetric gain-loss Hamiltonian in Eq. (4.1) in different regimes: the broken phase, $g = 0.2 < b$, with PHRE (a) and GLE (c) and the unbroken phase , $g = 3 > b$, with PHRE (b) and GLE (d).Other parameters are $a = 0, b = 2, T = 4, J(\omega) = 0.005\omega$.

Exceptional Points

Hamiltonian (Liouvillian) dynamics is governed by $e^{-i\hat{H}t}|\psi(t_0)\rangle$ ($e^{\mathcal{L}t}|\psi(t_0)\rangle$ so the elements of the system density matrix is given by $\sum_i c_i e^{\lambda \mathcal{L}_i t}$ where c_i depends on initial conditions) and therefore the eigenvalues of the Hamiltonian (Liouvillian) dictate the dynamics and (sometimes) the steady-state of the system, representing available dynamical modes. Non-hermitian systems, through a tunable parameter, can display characteristic modification of these modes (oscillatory or decaying, as observed prior) as signified by nondiagonalizabilities in parameter space called exceptional points. Exceptional points have become a hallmark of nonhermitian physics, with numerous nontrivial effects associated on their proximity. Crucially, temperature is an easily accessible parameter that has not been utilized to deform the eigenspectrum of the Liouvillian, in turn directing the position of exceptional points. This is because existing studies have without exception used the GKLS formalism, where temperature is not a microscopically tunable parameter.

In this work, we study the effects of temperature to the eigenspectrum of the pseudo-

density matrix Liouvillian (note that its eigenvalues are the same to the Liouvillian of the actual density matrix, see the next section). In Fig. (4.2), we plot the eigenvalues of the Hamiltonian Eq. (4.1) (circle marks) and the corresponding Liouvillian (no marks) as functions of the driving parameter g . Analytical details are presented in the next section. The third order HEP becomes a second order LEP once the system is open to the environment. It is also shifted from the original position, similar to the observations in Refs. [23, 28].

In the PHRE formalism, the eigenvalues of the Liouvillian is obtained through an effective description of the system in the energy basis, where the system Hamiltonian becomes entirely real (in the unbroken phase) or with complex conjugate eigenvalue pairs (in the broken phase). The nonhermiticity is delegated to the system interaction operator \hat{S} which becomes nonhermitian in the energy basis. It was pointed out in Refs. [75, 76] in the context of photonic devices that complex couplings may lead to the displacements of EPs in parameter space, in agreement to our observation here.

In addition to temperature, with the PHRE formalism the rates themselves bifurcate as a function of g . Further, the imaginary part of the generalized spectral density may also be engineered to deform the eigenspectrum of the Liouvillian, as we discuss further in the section after next.

Additional details on analyzing the Liouvillian

We defined the Liouvillian operating on the vectorized pseudo-density matrix. This is explicitly

$$\begin{bmatrix} \sigma_{11} & \sigma_{12} \\ \sigma_{21} & \sigma_{22} \end{bmatrix} \begin{bmatrix} \eta_{11} & \eta_{12} \\ \eta_{21} & \eta_{22} \end{bmatrix} = \begin{bmatrix} \sigma_{11}\eta_{11} + \sigma_{12}\eta_{21} & \sigma_{11}\eta_{12} + \sigma_{12}\eta_{22} \\ \sigma_{21}\eta_{11} + \sigma_{22}\eta_{21} & \sigma_{21}\eta_{12} + \sigma_{22}\eta_{22} \end{bmatrix} \rightarrow \begin{bmatrix} \sigma_{11}\eta_{11} + \sigma_{12}\eta_{21} \\ \sigma_{11}\eta_{12} + \sigma_{12}\eta_{22} \\ \sigma_{21}\eta_{11} + \sigma_{22}\eta_{21} \\ \sigma_{21}\eta_{12} + \sigma_{22}\eta_{22} \end{bmatrix} \quad (4.6)$$

what we would like is a Liouvillian operating on $[\sigma_{11} \ \sigma_{12} \ \sigma_{21} \ \sigma_{22}]^T$ and so we find M so that

$$\begin{bmatrix} \sigma_{11}\eta_{11} + \sigma_{12}\eta_{21} \\ \sigma_{11}\eta_{12} + \sigma_{12}\eta_{22} \\ \sigma_{21}\eta_{11} + \sigma_{22}\eta_{21} \\ \sigma_{21}\eta_{12} + \sigma_{22}\eta_{22} \end{bmatrix} = M \begin{bmatrix} \sigma_{11} \\ \sigma_{12} \\ \sigma_{21} \\ \sigma_{22} \end{bmatrix}, \Rightarrow M = \begin{bmatrix} \eta_{11} & \eta_{21} & 0 & 0 \\ \eta_{12} & \eta_{22} & 0 & 0 \\ 0 & 0 & \eta_{11} & \eta_{21} \\ 0 & 0 & \eta_{12} & \eta_{22} \end{bmatrix} \quad (4.7)$$

and therefore

$$\begin{aligned} \dot{\vec{v}} &= M\dot{\vec{v}} = \tilde{\mathcal{L}}M\vec{v} \\ \Rightarrow \dot{\vec{v}} &= \underbrace{M^{-1}\tilde{\mathcal{L}}M}_{\mathcal{L}}\vec{v}, \end{aligned} \quad (4.8)$$

so the pseudo-Liouvillian is the similarity transform of the Liouvillian. Therefore they have the same set of eigenvalues. Similarly, a density matrix is rotated from/to the site basis via

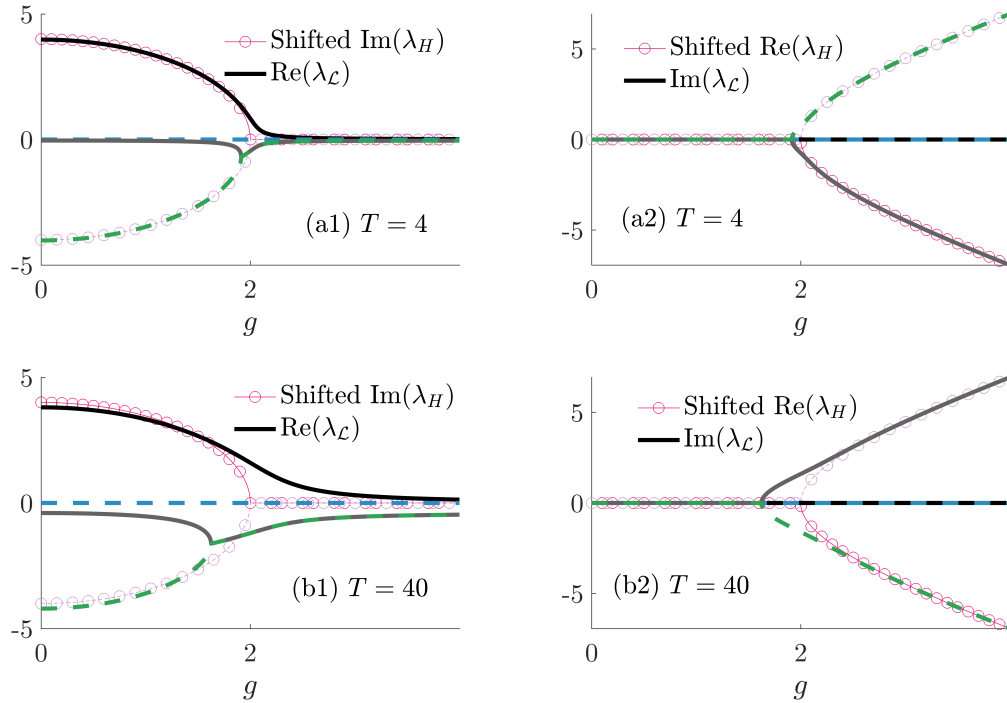


Figure 4.2: The eigenspectrum of the Hamiltonian and Liouvillian of the \mathcal{PT} -symmetric gain-loss Hamiltonian Eq. (4.1) open to a thermal environment via $\hat{S} = \hat{\sigma}_x$. In panel (a1) and (b1) we plot the imaginary part of the eigenvalues and in (a2) and (b2) the real parts. For panels (a1) and (a2), $T = 4$ and for (b1) and (b2), $T = 40$. Other parameters are: $a = 1, b = 2, J(\omega) = 0.005\omega$

a unitary transformation

$$\sigma^D = U\sigma^L U^\dagger \Rightarrow \exists \mathcal{U}, \text{s.t., } \vec{v}^D = \mathcal{U}\vec{v}^L. \quad (4.9)$$

Thus the eigenvalues of the pseudo-Liouvillian are the same with the Liouvillian in any basis. In the main thesis, we analyzed the eigenspectrum of the pseudo-Liouvillian.

In particular for the system Eq. (4.1) we analyze the Liouvillian as follows. The pseudo density matrix, vectorized as $\vec{v} = [\tilde{\sigma}_{11} \ \tilde{\sigma}_{21} \ \tilde{\sigma}_{12} \ \tilde{\sigma}_{22}]^T$, follows

$$\dot{\vec{v}}(t) = \mathcal{L}\vec{v}(t), \quad (4.10)$$

where

$$\begin{aligned} \mathcal{L}(1,1) &= -S_{12}^D S_{21}^D k_{1 \rightarrow 2}, \quad \mathcal{L}(1,2) = \frac{\gamma(S_{11}^D S_{21}^D - S_{12}^D S_{22}^D)}{2\beta}, \\ \mathcal{L}(1,3) &= \frac{\gamma(S_{11}^D S_{21}^D - S_{12}^D S_{22}^D)}{2\beta}, \quad \mathcal{L}(1,4) = \frac{1}{2}(k_{1 \rightarrow 2}(S_{21}^D)^2 + k_{2 \rightarrow 1}(S_{12}^D)^2) \end{aligned}$$

$$\begin{aligned}
 \mathcal{L}(2,1) &= \frac{(S_{11}^D - S_{22}^D)S_{21}^D k_{1\rightarrow 2}}{2} + \frac{(S_{12}^D - S_{21}^D)S_{11}^D \gamma}{2\beta}, \\
 \mathcal{L}(2,2) &= \frac{\gamma S_{11}^D S_{22}^D - (S_{22}^D)^2/2 - (S_{11}^D)^2/2}{\beta} - \frac{S_{12}^D S_{21}^D}{2}(k_{1\rightarrow 2} + k_{2\rightarrow 1}) + 8i\sqrt{\gamma^2 - b^2}, \\
 \mathcal{L}(2,3) &= \frac{1}{2}(k_{1\rightarrow 2}(S_{21}^D)^2 + k_{2\rightarrow 1}(S_{12}^D)^2), \\
 \mathcal{L}(2,4) &= \frac{(S_{22}^D - S_{11}^D)S_{12}^D k_{2\rightarrow 1}}{2} + \frac{(S_{21}^D - S_{12}^D)S_{22}^D \gamma}{2\beta}, \\
 \mathcal{L}(3,1) &= \frac{(S_{11}^D - S_{22}^D)S_{21}^D k_{1\rightarrow 2}}{2} + \frac{(S_{12}^D - S_{21}^D)S_{11}^D \gamma}{2\beta}, \quad \mathcal{L}(3,2) = \frac{1}{2}(k_{1\rightarrow 2}(S_{21}^D)^2 + k_{2\rightarrow 1}(S_{12}^D)^2), \\
 \mathcal{L}(3,3) &= \frac{\gamma S_{11}^D S_{22}^D - (S_{22}^D)^2/2 - (S_{11}^D)^2/2}{\beta} - \frac{S_{12}^D S_{21}^D}{2}(k_{1\rightarrow 2} + k_{2\rightarrow 1}) - 8i\sqrt{\gamma^2 - b^2}, \\
 \mathcal{L}(3,4) &= \frac{(S_{22}^D - S_{11}^D)S_{12}^D k_{2\rightarrow 1}}{2} + \frac{(S_{21}^D - S_{12}^D)S_{22}^D \gamma}{2\beta}, \quad \mathcal{L}(4,1) = S_{12}^D S_{21}^D k_{1\rightarrow 2}, \\
 \mathcal{L}(4,2) &= -\frac{\gamma(S_{11}^D S_{21}^D - S_{12}^D S_{22}^D)}{2\beta}, \quad \mathcal{L}(4,3) = -\frac{\gamma(S_{11}^D S_{21}^D - S_{12}^D S_{22}^D)}{2\beta}, \quad \mathcal{L}(4,4) = -S_{12}^D S_{21}^D k_{2\rightarrow 1}.
 \end{aligned} \tag{4.11}$$

with $S^D = V\sigma_x V^{-1}$ where the columns of the matrix V are composed of the eigenvectors of the system Hamiltonian Eq. (4.1). This Liouvillian is constructed out of the Redfield tensor.

Additional simulations

Here we present calculations which are interesting but due to time constraints discussions warranted are delegated to a future work.

Varying the imaginary frequency spectral density

Here we adopt a damped complex spectral density, $J^G(\omega_R, \omega_I) = J(\omega_R)e^{-\zeta\omega_I}$ with $\zeta = 1$. It is observed in Fig. (4.3) that the eigenspectrum of the Liouvillian analogous to that in Fig. (4.2) is deformed nontrivially.

Varying the system-bath coupling parameter

Here we show in Fig. (4.4) that the system bath coupling parameter (and equivalently e.g., the slope of the Ohmic spectral density) acts similarly to temperature in shifting the LEP. However, temperature is still a much more accessible parameter to tune experimentally.

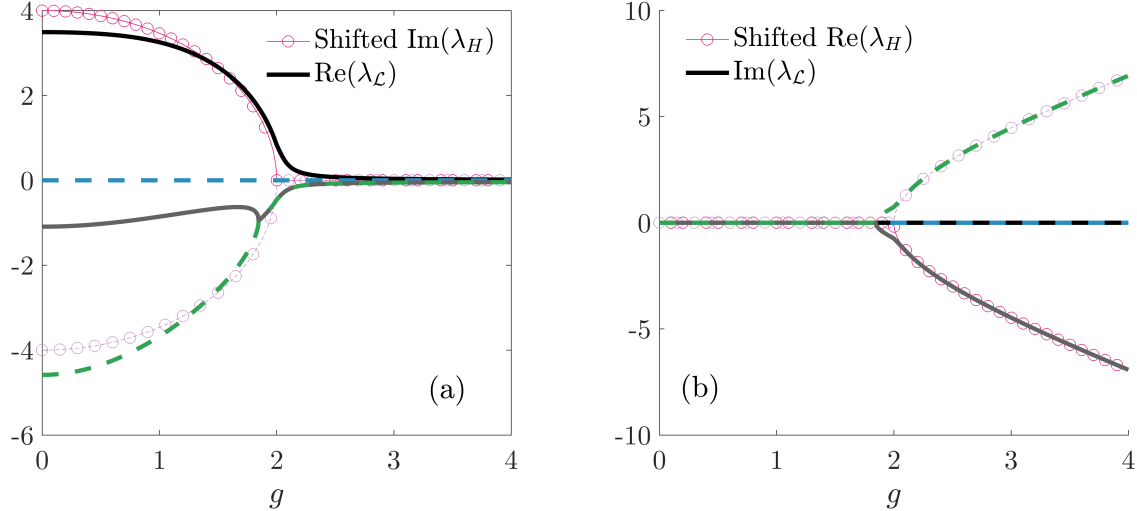


Figure 4.3: Liouvillian eigenspectrum of the \mathcal{PT} -symmetric gain-loss Hamiltonian Eq. (4.1) calculated using PHRE, with a modified generalized spectral density. Parameters: $a = 0, b = 2, T = 4, J^G(\omega_R, \omega_I) = 0.005\omega_R e^{-\omega_I}$.

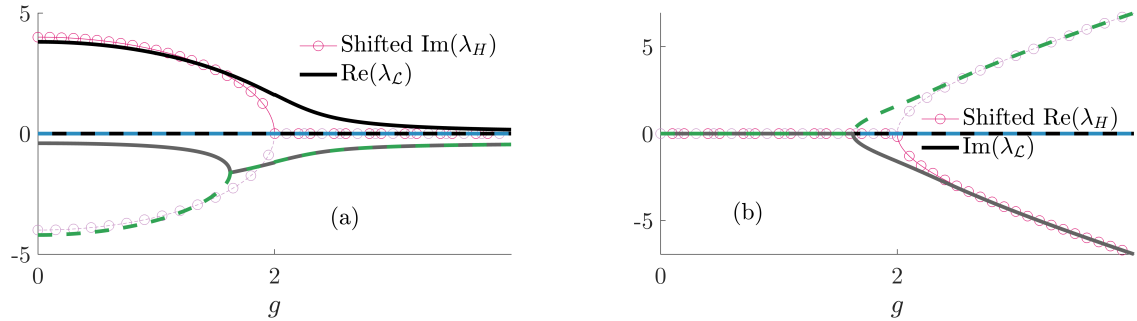


Figure 4.4: Liouvillian eigenspectrum of the \mathcal{PT} -symmetric gain-loss Hamiltonian Eq. (4.1) calculated using PHRE, with a modified Ohmic spectral density slope. Parameters: $a = 0, b = 2, T = 4, J^G(\omega_R, \omega_I) = 0.05\omega_R$.

Superohmic baths

In most cases, bosonic baths can be described by power-law spectral densities of the form [77],

$$J(\omega) = \gamma \frac{\omega^s}{\omega_{ph}^{s-1}} e^{-\omega/\omega_c}, \quad (4.12)$$

with cutoff frequency ω_c and phononic frequency ω_{ph} . In the main text, we set $s = 1$ so that the bath is ohmic, although it is also perfectly reasonable to have subohmic ($s < 1$) or superohmic ($s > 1$) baths. Interestingly, for superohmic baths, the usual term respon-

sible for dephasing in Eq. (2.35), $\pi \lim_{\omega \rightarrow 0^+} J(\omega)n(|\omega|)$, vanishes. In Fig. 4.5 we plot the eigenspectrum of a superohmic bath, setting $\omega_{ph} = \omega_c$, and observe that it matches the Hamiltonian eigenspectrum without LEPs being displaced. This highlights the importance of a nonvanishing dephasing term.

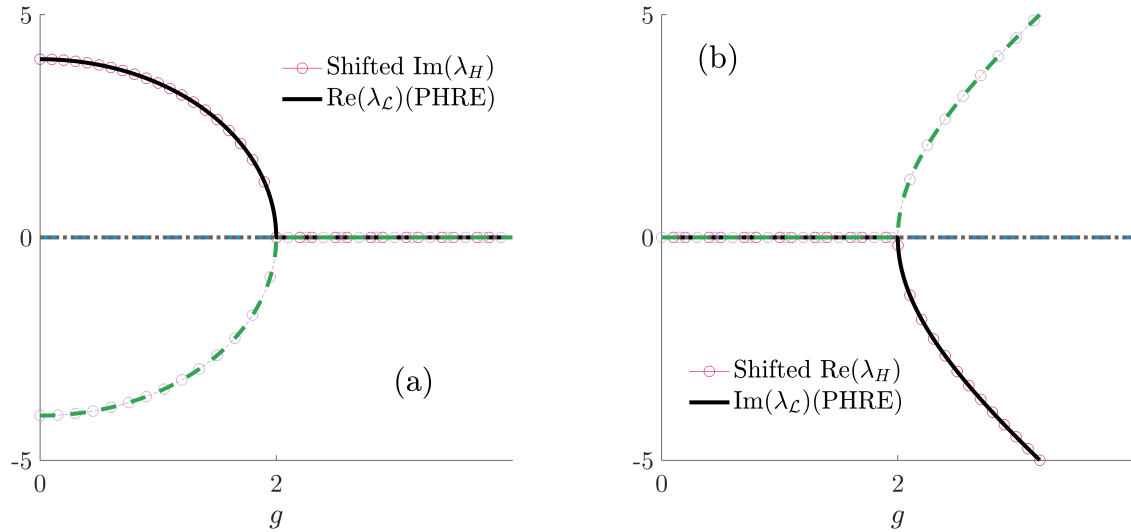


Figure 4.5: Liouvillian eigenspectrum of the \mathcal{PT} -symmetric gain-loss Hamiltonian Eq. (4.1) calculated using PHRE, with a superohmic spectral density (and the imaginary part set to 1). Parameters: $a = 0, b = 2, T = 4, J^G(\omega_R, \omega_I) = \frac{\gamma}{\omega_c} \omega_R^2, \gamma = 0.005, \omega_c = 10000$.

Chapter 5

Applications C: Three-level gain-loss \mathcal{PT} -symmetric Hamiltonian

Here we consider a three-level quantum system: two degenerate excited states experiencing either gain or loss, thermally and symmetrically coupled to a common ground state. Compared to the two level \mathcal{PT} -symmetric Hamiltonian, here thermal effects are less interlaced from nonhermitian effects and in principle manifestations of nonsecular effects can be observed far from the exceptional point. The Hamiltonian of this model reads

$$\hat{H}_S = \begin{bmatrix} \epsilon_1 & 0 & 0 \\ 0 & a - ib & g \\ 0 & g & a + ib \end{bmatrix}, \quad \hat{S} = \begin{bmatrix} 0 & 1 & 1 \\ 1 & 0 & 0 \\ 1 & 0 & 0 \end{bmatrix} \quad (5.1)$$

with metric

$$\eta = \begin{bmatrix} 1 & 0 & 0 \\ 0 & 0 & 1 \\ 0 & 1 & 0 \end{bmatrix}, \quad (5.2)$$

where $\epsilon_1 < a$. This and related models have been observed to exhibit a number of interesting effects, e.g., \mathcal{PT} -symmetric Talbot effect [78]. In the context of this work, the dynamics of this model is expected to exhibit the interplay of (1) thermal effects since relaxation and excitation rates from (to) the ground state (excited state) are different and related by detailed balance, (2) nonhermitian effects (gain and loss of the excited states), and (3) nonsecular behaviour.

In Figure (5.1) we plot the open system dynamics using PHRE ($\epsilon_1 = 0 < a = 1, b = 2$), prepared in the maximally entangled state $\sigma(0) = \mathbf{1}/3$ (not an eigenstate). In panel (a) we set $g = 0.2 < b$, so the system is in the broken phase. Here, steady state solutions depend on the initial state, characteristic of degenerate V -models with symmetric couplings [79]. This is emulated in our pseudo-hermitian V -model in the broken phase, since the generalized spectral density was chosen to be insensitive to imaginary Bohr frequencies. We present

an analytical analysis in the next section for the case when $a = g = 0$. It shows that as expected, for large enough b the third level continuously gains populations while the second level decays to zero. Since here the second and third levels are coupled only indirectly (through the ground state), at long times essentially only the third level is populated. Note, the relative populations of the ground compared to the excited levels can be adjusted by tuning the bias of the relaxation and excitation rates, either through changing temperature or the ground-excited splitting energy a (see Additional Simulations). In panel (b), the system is in the unbroken phase as signified by pronounced transient oscillations. Notably, excited states relax to approximately equal populations. This because the larger coupling term g constantly interchanges the populations of the excited states, overpowering the asymmetry induced by spontaneous gain or loss through the b term. Both nonhermitian decay and thermal relaxation contribute to damping oscillatory dynamics.

Finally, in panel (c) we show the dynamics close to the (Hamiltonian) exceptional point $g \approx b$, meaning interlevel coupling somewhat balances out spontaneous gain and loss. Therefore the excited states still relax to distinguishable steady states, but with little to no oscillation. The fact that the steady state population of the ground state is lesser than the excited states is due to the splitting a which is considered small here. In Additional Simulations we show that (1) the parameters a, b, g can be each tuned to obtain a particular steady state, and (2) that this model can display prethermalization behaviour [80] as $b \rightarrow 0$. Notably, the novel observation is that the quasi-degeneracy of the V-model, which breaks the integrability of the degenerate V-model and induces prethermalization, is here replaced by a small gain-loss parameter b .

In Fig. (5.2) we show the eigenspectrum of the three-level system. This shares some similarities with the two-level analog shown in Fig. (4.2) although crucially, here the opening the system to a thermal environment results to the subjugation of exceptional points. The transition from the broken to unbroken phase or vice-versa, that is as eigenmodes coalesce, occurs smoothly and very gradually. This was similarly observed in e.g., Ref. [81]. Furthermore, here we observe an avoided crossing past the HEP.

Analytical results when $g = 0$

Here, the system is already diagonal so we can write the equations of motion (from PHRE) of the pseudo-density matrix as (assuming the state is prepared without imaginary coherences)

$$\begin{aligned} \dot{\tilde{\sigma}}_{11}(t) &= -(k_{1 \rightarrow 2} + k_{1 \rightarrow 3})\tilde{\sigma}_{11}(t) + k_{2 \rightarrow 1}\tilde{\sigma}_{22}(t) + k_{3 \rightarrow 1}\tilde{\sigma}_{33}(t) \\ &\quad + \frac{(k_{2 \rightarrow 1} + k_{3 \rightarrow 1})}{2}(\tilde{\sigma}_{23}(t) + \tilde{\sigma}_{32}(t)), \end{aligned} \quad (5.3)$$

$$\dot{\tilde{\sigma}}_{22}(t) = (k_{1 \rightarrow 2})\tilde{\sigma}_{11}(t) - k_{2 \rightarrow 1}\tilde{\sigma}_{22}(t) - \frac{k_{2 \rightarrow 1}}{2}(\tilde{\sigma}_{23}(t) + \tilde{\sigma}_{32}(t)), \quad (5.4)$$

$$\dot{\tilde{\sigma}}_{33}(t) = (k_{1 \rightarrow 3})\tilde{\sigma}_{11}(t) - k_{3 \rightarrow 1}\tilde{\sigma}_{33}(t) - \frac{k_{3 \rightarrow 1}}{2}(\tilde{\sigma}_{23}(t) + \tilde{\sigma}_{32}(t)), \quad (5.5)$$

$$\dot{\tilde{\sigma}}_{32}(t) = 2b\tilde{\sigma}_{32}(t) - \frac{1}{2}(k_{2 \rightarrow 1} + k_{3 \rightarrow 1})\tilde{\sigma}_{32}(t)$$

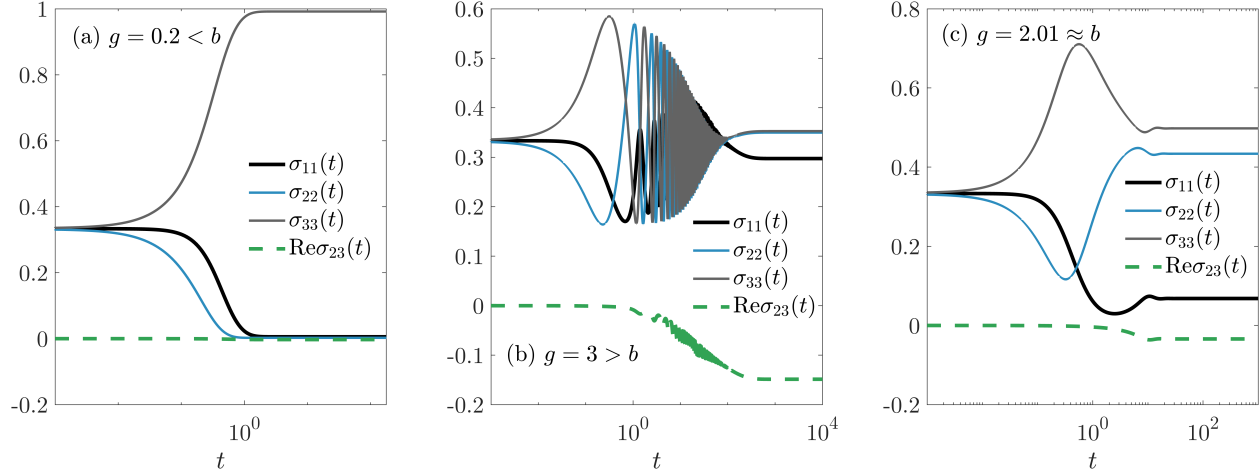


Figure 5.1: Dynamical evolution of the density matrix of the dissipative three-level V-model Hamiltonian using PHRE prepared in the maximally entangled state $\sigma(0) = \frac{1}{3}\mathbf{1}$. We vary the driving parameter g across panels, (a) $g = 0.2$ (broken phase), (b) $g = 3$ (unbroken phase), and (c) $g = 2.01$ (close to the exceptional point). Other parameters are $\epsilon_1 = 0, a = 1, b = 2, T = 4, J(\omega) = 0.005\omega$.

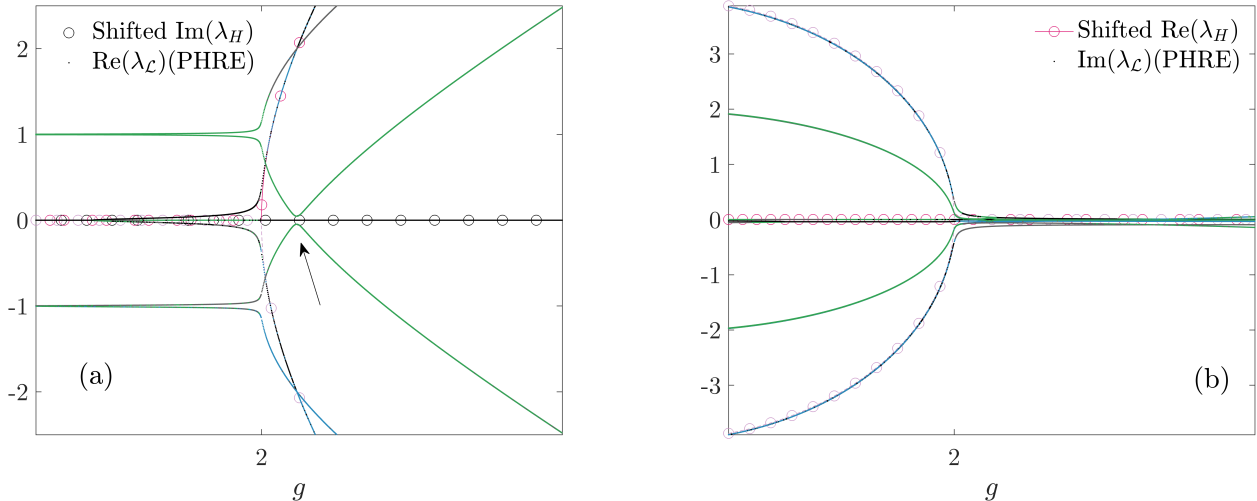


Figure 5.2: The eigenspectrum of the Liouvillian open to a thermal environment Eq. (5.1). In panel (a) we plot the imaginary part of the eigenvalues and in (b) the real parts. The arrow indicate an avoided crossing. Other parameters are: $a = 0, b = 2, T = 4, J(\omega) = 0.005\omega$

$$\begin{aligned} -\frac{1}{2}k_{2 \rightarrow 1}\tilde{\sigma}_{22}(t) - \frac{1}{2}k_{3 \rightarrow 1}\tilde{\sigma}_{33}(t) + \frac{1}{2}(k_{1 \rightarrow 2} + k_{1 \rightarrow 3})\tilde{\sigma}_{11}(t), \\ \dot{\tilde{\sigma}}_{23}(t) = -2b\tilde{\sigma}_{23}(t) - \frac{1}{2}(k_{2 \rightarrow 1} + k_{3 \rightarrow 1})\tilde{\sigma}_{23}(t) \end{aligned} \quad (5.6)$$

$$-\frac{1}{2}k_{2\rightarrow 1}\tilde{\sigma}_{22}(t) - \frac{1}{2}k_{3\rightarrow 1}\tilde{\sigma}_{33}(t) + \frac{1}{2}(k_{1\rightarrow 2} + k_{1\rightarrow 3})\tilde{\sigma}_{11}(t). \quad (5.7)$$

Assuming that the generalized spectral density does not depend on the imaginary part of the Bohr frequencies, $k_{3\rightarrow 1} = k_{2\rightarrow 1} \equiv k_\downarrow$ so

$$\dot{\tilde{\sigma}}_{11}(t) = -2k_\uparrow\tilde{\sigma}_{11}(t) + 2k_\downarrow\underbrace{(\tilde{\sigma}_{22}(t) + \tilde{\sigma}_{33}(t))}_{\tilde{P}_e(t)} + k_\downarrow(\tilde{\sigma}_{23}(t) + \tilde{\sigma}_{32}(t)) \quad (5.8)$$

$$\dot{\tilde{P}}_e(t) = 2k_\uparrow\tilde{\sigma}_{11}(t) - 2k_\downarrow\tilde{P}_e(t) - k_\downarrow(\tilde{\sigma}_{23}(t) + \tilde{\sigma}_{32}(t)) \quad (5.9)$$

$$\dot{\tilde{\sigma}}_{32}(t) = 2b\tilde{\sigma}_{32}(t) - k_\downarrow\tilde{\sigma}_{32}(t) - k_\downarrow\tilde{P}_e(t) + k_\uparrow\tilde{\sigma}_{11}(t) \quad (5.10)$$

$$\dot{\tilde{\sigma}}_{23}(t) = -2b\tilde{\sigma}_{23}(t) - k_\downarrow\tilde{\sigma}_{23}(t) - k_\downarrow\tilde{P}_e(t) + k_\uparrow\tilde{\sigma}_{11}(t) \quad (5.11)$$

and thus

$$\frac{d}{dt}\tilde{\vec{v}}(t) = \underbrace{\begin{bmatrix} -2k_\uparrow & 2k_\downarrow & k_\downarrow & k_\downarrow \\ 2k_\uparrow & -2k_\downarrow & -k_\downarrow & -k_\downarrow \\ k_\uparrow & -k_\downarrow & 2b - k_\downarrow & 0 \\ k_\uparrow & -k_\downarrow & 0 & -2b - k_\downarrow \end{bmatrix}}_M \tilde{\vec{v}}(t) \quad (5.12)$$

where $\tilde{\vec{v}} \equiv [\tilde{\sigma}_{11}(t) \ \tilde{P}_e(t) \ \tilde{\sigma}_{32}(t) \ \tilde{\sigma}_{23}(t)]^T$. The coefficient matrix in Eq. (5.12) is singular, and the dynamics it dictates has infinitely many steady-state solutions. We can still conclude a few important observations here. First, note that to revert to the (actual) density matrix we multiply the pseudo density matrix by the inverse of the metric η . Here this simply rearranges its elements, namely $\tilde{\sigma}_{23} \rightarrow \sigma_{22}$ and $\tilde{\sigma}_{32} \rightarrow \sigma_{33}$. Thus, looking at the equations of motion, when $2b > k_\downarrow$ the third level continuously gains population. On the other hand the second level (with the loss term) steadily decays.

This is expected, but this analysis makes clear that the PHRE models decaying dynamics through using the additional degree of freedom of the coherences (can be negative and no trace constraints).

Additional simulations

Long-lived nonhermitian dynamics

A quasi-degenerate three level model [56, 80] has been known to exhibit prethermalization behaviour, with dynamics lifetime scaling square-inversely proportional to the quasidegenerate splitting energy [82, 83]. Here we show that a degenerate nonhermitian system can also display prethermalization behaviour, with the breaking of integrability delegated to the small but nonvanishing gain-loss parameter.

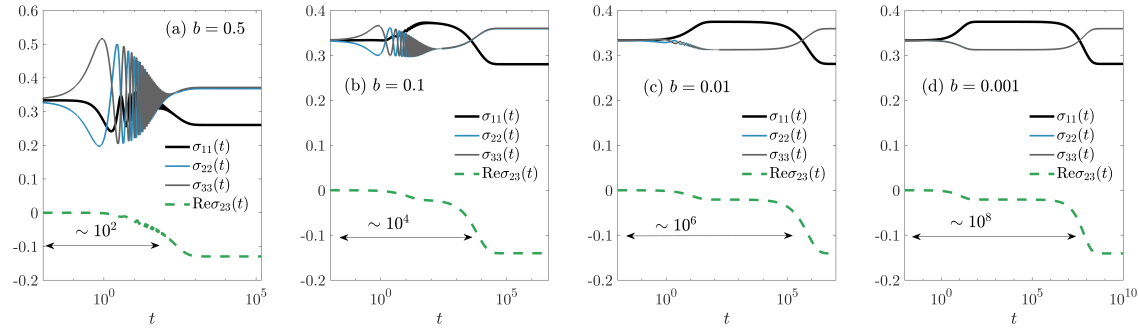


Figure 5.3: (No thermal bias) Dynamical evolution of the density matrix of the dissipative three-level V-model Hamiltonian using PHRE prepared in the maximally entangled state $\sigma(0) = \frac{1}{3}\mathbf{1}$. We vary the gain-loss parameter b across panels, (a) $b = 0.5$, (b) $b = 0.1$, (c) $b = 0.01$, and (d) $b = 0.001$. Other parameters are $\epsilon_1 = 0, b = 2, g = 1, T = 4, J(\omega) = 0.005\omega$.

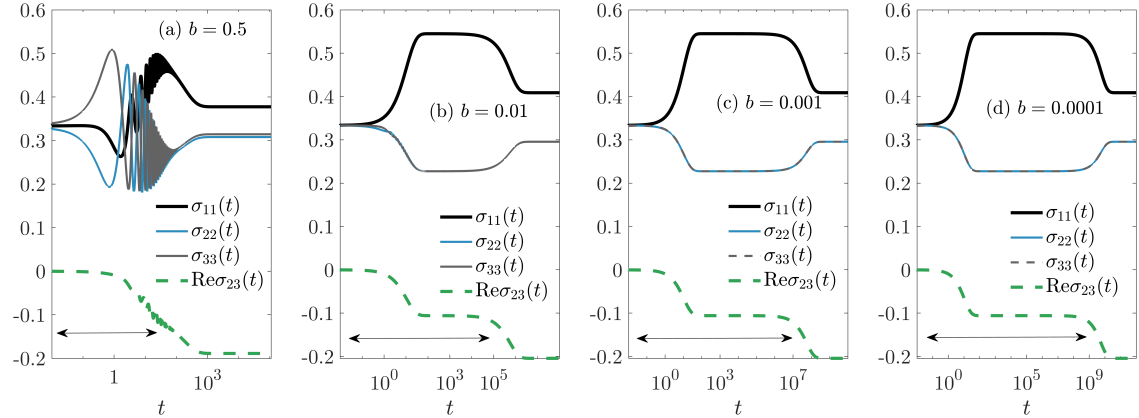


Figure 5.4: (High thermal bias) Dynamical evolution of the density matrix of the dissipative three-level V-model Hamiltonian using PHRE prepared in the maximally entangled state $\sigma(0) = \frac{1}{3}\mathbf{1}$. We vary the gain-loss parameter b across panels, (a) $b = 0.5$, (b) $b = 0.01$, (c) $b = 0.001$, and (d) $b = 0.0001$. Other parameters are $\epsilon_1 = 0, a = 5, g = 1, T = 4, J(\omega) = 0.005\omega$.

Where does the pseudohermitian system relax to?

In this section the particular Hamiltonian we discuss is the three level gain-loss \mathcal{PT} -symmetric Hamiltonian Eq. (5.1). This choice is due to the robustness of the model, with each parameters a, b, g , and T tunable to highlight thermal, nonhermitian decay, and interlevel coupling effects.

It must first be noted that while we would expect the system to relax to a thermal Gibbs state ($\sigma_{Gibbs} = \frac{e^{-\beta \hat{H}_s}}{\text{Tr}\{e^{-\beta \hat{H}_s}\}}$) for $b = 0$, this is not always true. Indeed, when $b = 0$ with the Hamiltonian Eq. (5.1), the system is integrable and therefore it suffers from having infinitely

many steady-state solutions depending on the initial state. While the integrability can be broken by introducing a small splitting between the excited states, this would cause the Hamiltonian to violate the pseudohermiticity condition $\hat{H}^\dagger = \eta \hat{H} \eta^{-1}$. Instead, we make use of our recent finding that a small b can be used to break integrability, causing the system to relax to the "true" steady state with characteristic lifetime proportional to b^{-2} . Essentially, the system will approach (but never fully reach) the Gibbs state in the limit of small but nonzero b , specifically $0 < b \ll a, g, \beta$. We plot this analysis in Fig. (5.5). Note that for $b < g$ such that the system is in the broken phase, the Gibbs state is itself ill defined due to complex eigenenergies.

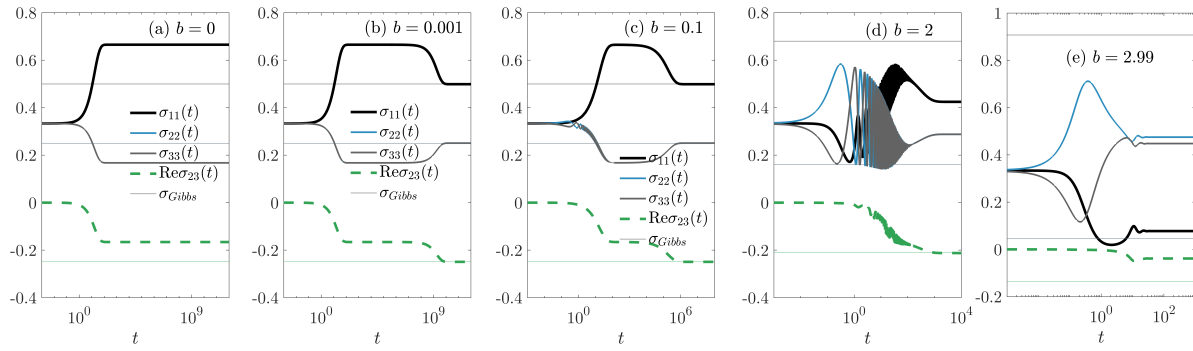


Figure 5.5: Dynamical evolution of the density matrix of the dissipative three-level V-model Hamiltonian using PHRE prepared in the maximally entangled state $\sigma(0) = \frac{1}{3}\mathbf{1}$. We vary the gain-loss parameter b across panels, (a) $b = 0$, (b) $b = 0.001$, (c) $b = 0.1$, (d) $b = 2$, and (e) $b = 2.99$. Other parameters are $\epsilon_1 = 0$, $a = 3$, $g = 3$, $T = 1$, $J(\omega) = 0.005\omega$.

Dynamical impacts of varying temperature

Here we show briefly the impacts of changing temperature on the dynamics of pseudohermitian systems specifically for the three level gain-loss \mathcal{PT} -symmetric Hamiltonian Eq. (5.1). Primarily, temperature controls the relative populations of the ground and excited states. This is summarized in Fig. (5.6).

Analysis in the eigenbasis

Here we briefly discuss dynamics of the three level gain-loss \mathcal{PT} -symmetric Hamiltonian Eq. (5.1) in its eigenbasis. It must be noted that although in the unbroken regime eigenenergies are real, **even for unitary dynamics** (i.e., no coupling to a thermal bath) one cannot expect physical density matrices in both the energy and local basis simultaneously. This is because the basis change matrix is complex, therefore if we demand the local basis density matrix e.g., to have strictly real diagonal elements, generally in the energy basis they will be complex (i.e., with nonzero imaginary populations). Note that in some parameter regimes one may even get negative eigenbasis populations. Regardless, we plot in Fig. 5.7 the

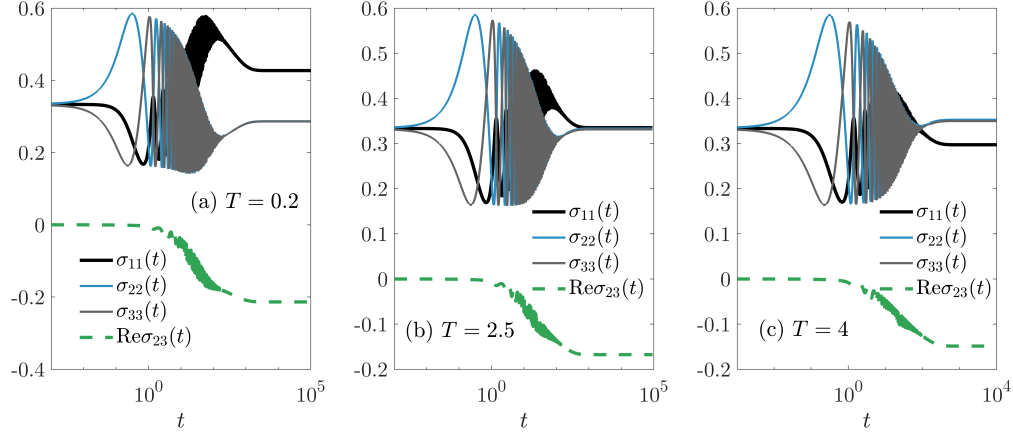


Figure 5.6: Dynamical evolution of the density matrix of the dissipative three-level V-model Hamiltonian using PHRE prepared in the maximally entangled state $\sigma(0) = \frac{1}{3}\mathbf{1}$. We vary the temperature T across panels, (a) $T = 0.2$, (b) $T = 2.5$, and (e) $T = 4$. Other parameters are $\epsilon_1 = 0$, $a = 1$, $g = 3$, $b = 2$, $J(\omega) = 0.005\omega$.

dynamics of the density matrix elements in the energy basis for two differing regimes. We show that as b increases (1) the steady state density matrix further deviates from the Gibbs state, and (2) accumulates more transient imaginary populations. One would expect for this model that the coherences decay to zero, but interestingly this is also only observed for small b .

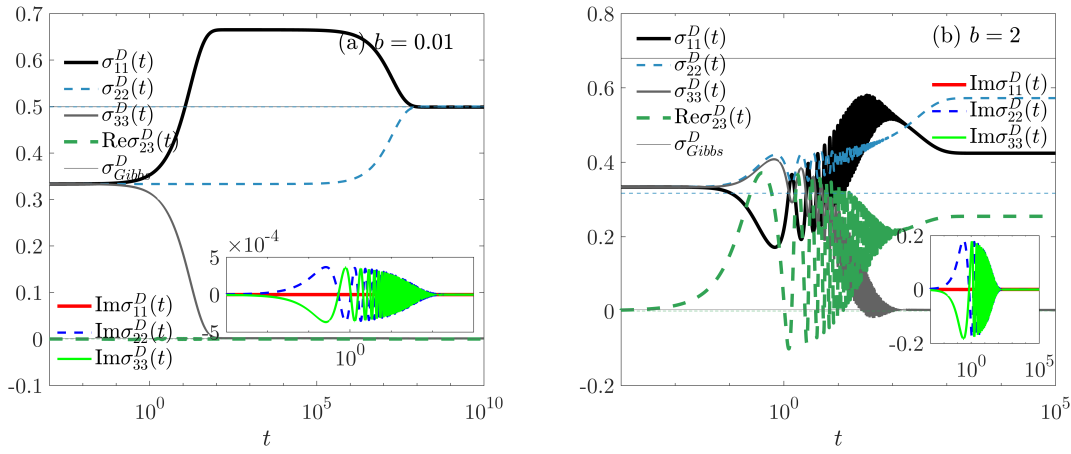


Figure 5.7: Dynamical evolution of the density matrix (in the energy basis) of the dissipative three-level V-model Hamiltonian using PHRE prepared in the maximally entangled state $\sigma(0) = \frac{1}{3}\mathbf{1}$. We vary b across panels, (a) $b = 0.01$, and (b) $b = 2$. Insets show imaginary populations. Other parameters are $\epsilon_1 = 0$, $a = 1$, $g = 3$, $T = 1$, $J(\omega) = 0.005\omega$.

Chapter 6

Discussion and Outlook

We have developed a nonsecular master equation framework to model pseudo-hermitian Hamiltonians open to a thermal environment. This approach makes use of the pseudo-density matrix $\tilde{\rho}(t) = \rho(t)\eta$ where $\hat{H}^\dagger = \eta\hat{H}\eta^{-1}$, which allows performing the usual Born-Markov perturbation scheme. The resulting equation takes the Redfield form, and therefore existing tools which expands on the Redfield equation are applicable. These include Polaron transformations [84, 85, 86], the reaction-coordinate mapping [87, 88], and a number of refined Redfield methods [89]. The tactic through which PHRE simulates dynamics with spontaneous gain/loss is by mapping populations to coherences and vice versa, via $\sigma \leftrightarrow \sigma\eta$, since bare Born-Markov Redfield cannot model spontaneous decay. Through this, population dynamics gain additional degrees of freedom as coherences are not constrained by positivity and trace conditions (see analytical analysis in Ch. 4).

Our approach differs from the usual methods to study LEPs in the literature as we treat the nonhermiticity of the system Hamiltonian fully microscopically. This yields two fundamental insights: (1) both temperature and the coupling parameter (or e.g., the slope of the Ohmic spectral density function) can be tuned to deform the eigenspectrum, in turn displacing the position of exceptional points in parameter space. Temperature is typically easier to control than the coupling parameter. (2) In the broken regime, the spectral density of the bath needs to be generalized to solve the relevant Laplace transform. Here, we introduced a simple fix via complex delta functions but a more systematic derivation is to follow as a future study. Regardless, the imaginary part of the generalized spectral density is an unprobed degree of freedom that can have interesting implications both on dynamics and on the eigenspectrum. In addition, even the real part of the spectral density may have nontrivial effects to the eigenspectrum of the Liouvillian: while here we used an Ohmic spectral density, where $\lim_{\omega \rightarrow 0^+} J(\omega)n(|\omega|) \neq 0$, this relationship is not general. When this quantity vanishes (corresponding to superohmic baths), PHRE does not predict displacements of exceptional points. Throughout this study, nontrivial nonsecular effects did not emerge far or close to the EPs. Finally, we mention the last piece of approximation made for the numerics in this work, that is to set the imaginary part of the bath correlation function Laplace transform to zero. It was argued in Ref. [56] that this quantity is far

smaller than the real part for Ohmic baths and further that they contribute only to Lamb shift, justifying our choice here. However, mixed terms (e.g., imaginary part of the bath correlation function Laplace transform with the imaginary part of the coupling matrix in the eigenbasis and vice versa) may admittedly lead to nontrivial behaviour. More detailed investigation is left for a future study.

While here we focused on pseudo-hermitian quantum systems, analogous derivation may be undertaken to generalize the results to all *nonhermitian* quantum systems. We sketch the approach in the appendix. Regardless, pseudo-hermitian hamiltonians already encompass a wide variety of quantum systems open to a thermal environment. Interesting topics for following studies include the impacts of nonequilibrium effects, exploiting proximities to exceptional points for dynamical acceleration [90, 80], and further investigating the positivity and nonlinearity of the PHRE. Future plans are focused on analytically solving nonhermitian dynamics with methods described in e.g., Ref. [80]. This work paves the way for experimental studies of pseudo-hermitian quantum systems with temperature as a tunable parameter, with potential applications in quantum sensing, quantum information sciences, and quantum control. Further, this work opens up the possibility of studying pseudohermitian Hamiltonians, an often overlooked class of systems, interacting with a thermal environment where microscopic details are important.

Appendix A

Pseudo-hermitian master equations in the Lindblad form

A completely positive trace preserving (CPTP) density matrix to density matrix map takes the Lindblad form ($\hbar \equiv 1$) [91]. In the energy basis,

$$\dot{\rho} = -i[\hat{H}, \rho] + \sum_k \Gamma_k \left(L_k \rho L_k^\dagger - \frac{1}{2} \{ L_k^\dagger L_k, \rho \} \right) \equiv \mathcal{L}\rho. \quad (\text{A.1})$$

To obtain an effective non-Hermitian description of the system, the quantum jump terms $\Gamma_k L_k \rho L_k^\dagger$ are dropped, yielding

$$\dot{\rho} = -i[\hat{H} - \underbrace{\frac{i}{2} \sum_k \Gamma_k L_k^\dagger L_k}_{\hat{H}_{\text{eff}}}, \rho] \equiv \mathcal{L}_{\text{eff}}\rho. \quad (\text{A.2})$$

A nonlinear term can be added to account for normalization [92], originating from the non-hermitian part

$$\frac{d}{dt} \text{tr}\{\rho\} = \frac{2}{i} \text{tr}\left(\rho \hat{H}_{nh}\right). \quad (\text{A.3})$$

Not discarding the quantum jump terms in Eq. (A.1) allows the investigation of Liouvillean exceptional points. However, both approaches still assume that the initial Hamiltonian is Hermitian. Recently, Refs. [39, 40, 41, 42] had modified the Lindblad equation to deal with pseudohermitian hamiltonians. Note that their approaches are distinct to what we develop in this work. Namely, our formalism is nonsecular and we treat the pseudohermiticity of our hamiltonian and the interaction with the thermal bath microscopically. Regardless, multiplying both sides of Eq. (A.1) with η gives

$$\dot{\tilde{\rho}} = -i[\hat{H}, \tilde{\rho}] + \sum_k \Gamma_k \left(L_k \tilde{\rho} L_k^\dagger - \frac{1}{2} \{ L_k^\dagger L_k, \tilde{\rho} \} \right), \quad (\text{A.4})$$

where $L_k^\ddagger = \eta^{-1} L^\dagger \eta$. This equation is most similar to our new formalism, so we used it to benchmark our results. Specifically, following Refs. [37, 38], we vectorize the density matrix as in the main text and define the Liouvillian as follows

$$\mathcal{L}_L = -i(\hat{H}_S \otimes \mathbf{1} - \mathbf{1} \otimes \hat{H}_S) + \sum_{\omega} k(\omega) \left(L_{\omega}^\ddagger \otimes L_{\omega} - \frac{1}{2} \{ L_{\omega}^\ddagger L_{\omega} \otimes \mathbf{1}, \mathbf{1} \otimes \mathbf{1} \} \right) \quad (\text{A.5})$$

with $k(\omega)$ chosen to match with the Redfield analog. Since the Generalized Lindblad approach is done in the local basis, ω are the energy differences between the diagonals. A few points of discussion are in order:

In Fig. (4.1), we compared the relaxation dynamics of the \mathcal{PT} -symmetric two-level Hamiltonian as predicted by PHRE and the Generalized Lindblad equation (GLE). In both the broken and unbroken phases away from the EP, both methods agree qualitatively in both the transient and steady-state regimes. Only very minor differences remain (e.g., in panel (d) the populations oscillate to very close to one and zero, which is not so pronounced in panel (b)). This is significant, as PHRE is done on the energy basis, where essentially the system Hamiltonian is Hermitian, while the system interaction operator is nonhermitian with complex elements. On the other hand, GLE is done on the local basis, where the system Hamiltonian is nonhermitian while the system interaction operator is hermitian with completely real elements. Even close to the HEP $g = b$ (Fig. (A.1)) both methods agree.

In Fig. (A.2), we plot the eigenspectra of the Liouvillians of the PHRE and of the analogous GLE. Both are very much identical except for one aspect: the GLE does not have the vanishing real part of the eigenvalue (blue crosses at the right panel). From numerical analysis it is found that this eigenvalue is proportional to the dephasing rate $\lim_{\omega \rightarrow 0^+} J(\omega)n(\omega)$. However, if we set $\lim_{\omega \rightarrow 0^+} J(\omega)n(\omega) = 0$ by hand, the eigenspectrum of the GLE simply reduces to the Hamiltonian eigenspectrum. A nonvanishing dephasing rate is crucial for the fully open Liouvillian (with quantum jump) description of the dynamics.

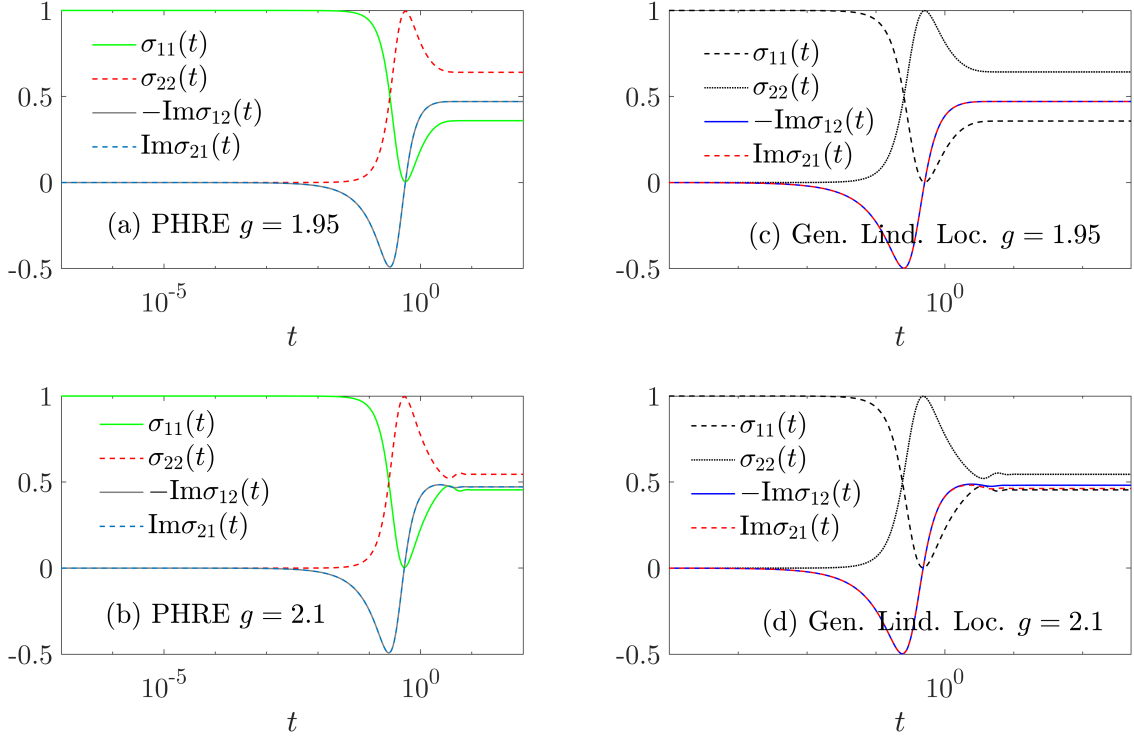


Figure A.1: Simulations of density matrix evolution of the \mathcal{PT} -symmetric gain-loss Hamiltonian Eq. (4.1) near the HEP, using PHRE (a) and (b) and GLE (c) and (d). Parameters: $a = 0, b = 2, T = 4, J(\omega) = 0.005\omega$.

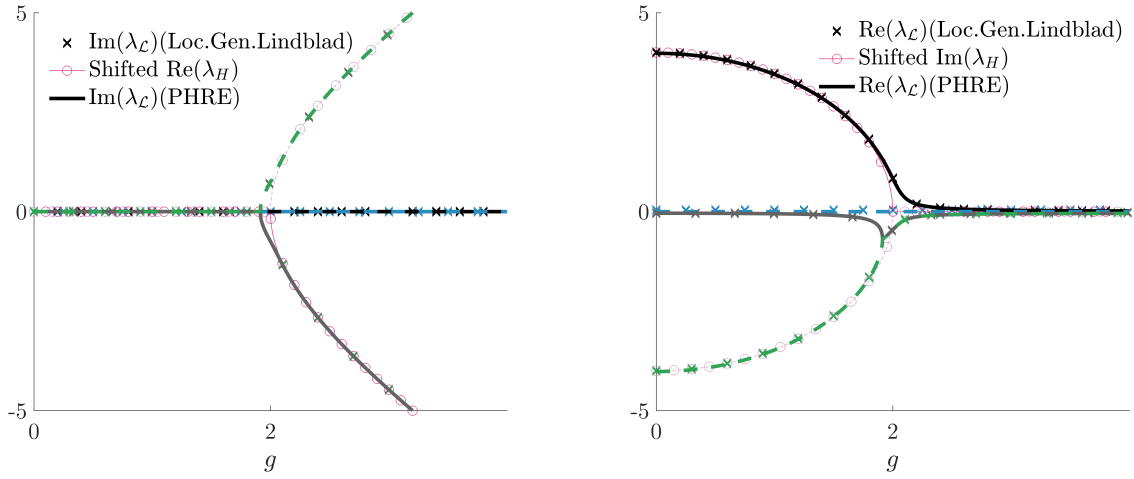


Figure A.2: Comparison of the Imaginary (left) and Real (right) part of the Liouvillian eigenspectrum of the \mathcal{PT} -symmetric gain-loss Hamiltonian Eq. (4.1) calculated using PHRE and GLE. Parameters: $a = 0, b = 2, T = 4, J(\omega) = 0.005\omega$.

Appendix B

Generalized Non-hermitian Redfield Master Equation

Starting from

$$\dot{\rho}(t) = \frac{1}{i\hbar}(\hat{H}\rho - \rho\hat{H}^\dagger) \quad (\text{B.1})$$

and with

$$\hat{H} = \underbrace{\hat{H}_S + \hat{H}_B}_{\hat{H}_0} + \hat{V}, \quad (\text{B.2})$$

we get

$$\begin{aligned} \dot{\rho}(t) &= \frac{1}{i\hbar}((\hat{H}_S + \hat{H}_B + \hat{V})\rho - \rho(\hat{H}_S^\dagger + \hat{H}_B^\dagger + \hat{V})) \\ &= \frac{1}{i\hbar}(\hat{H}_S\rho - \rho\hat{H}_S^\dagger + [\hat{H}_B + \hat{V}, \rho]) \end{aligned} \quad (\text{B.3})$$

Let us proceed to transform to an improper interaction picture. First,

$$\begin{aligned} \frac{\partial}{\partial t}(e^{i\hat{H}_0 t}\rho e^{-i\hat{H}_0^\dagger t}) &= e^{i\hat{H}_0 t}\frac{\partial \rho}{\partial t}e^{-i\hat{H}_0^\dagger t} + i\hat{H}_0 e^{i\hat{H}_0 t}\rho e^{-i\hat{H}_0^\dagger t} - ie^{i\hat{H}_0 t}\rho e^{-i\hat{H}_0^\dagger t}\hat{H}_0^\dagger \\ &= e^{i\hat{H}_0 t}\frac{\partial \rho}{\partial t}e^{-i\hat{H}_0^\dagger t} + i(\hat{H}_0\rho_I - \rho_I\hat{H}_0^\dagger) \\ &= e^{i\hat{H}_0 t}\frac{\partial \rho}{\partial t}e^{-i\hat{H}_0^\dagger t} + i(\hat{H}_S\rho_I - \rho_I\hat{H}_S^\dagger + [\hat{H}_B, \rho_I]) \end{aligned} \quad (\text{B.4})$$

hence

$$\dot{\rho}_I(t) = -i[\hat{V}_I, \rho_I] \quad (\text{B.5})$$

where the nonhermiticity is encoded when we transform back to the Schrödinger picture as $e^{iH_0 t}e^{-iH_0^\dagger t} \neq \mathbf{1}$. It may be possible to proceed from here to develop a generalization of the Redfield equation which is valid not only for pseudo-hermitian hamiltonians but for general nonhermitian hamiltonians. This remains a topic for future study.

Appendix C

Applications D: Asymmetric σ_y -type Hamiltonian

Dynamics

Another interesting prototypical PHH is an asymmetric σ_y -type Hamiltonian Eq. (C.1), this section highlights the emergence of some unphysical results when using the PHRE. The asymmetric σ_y -type Hamiltonian reads

$$\hat{H}_S = \begin{bmatrix} 0 & i \\ -i\gamma & 0 \end{bmatrix}, \quad \gamma \in \mathbb{R}. \quad (\text{C.1})$$

Here, $\eta = \hat{\sigma}_y$ and the eigenvalues are $\pm\sqrt{\gamma}$, therefore there is an exceptional point at $\gamma = 0$. Note that this two level Hamiltonian corresponds to a the motion of a simple harmonic oscillator with frequency γ [93]. The nondissipative dynamics is simple enough to solve analytically,

$$\langle 1 | \rho(t) | 1 \rangle = x \cos^2(\sqrt{\gamma}t) - \frac{(x-1) \sin^2(\sqrt{\gamma}t)}{\gamma}, \quad (\text{C.2})$$

$$\langle 2 | \rho(t) | 2 \rangle = \gamma x \sin^2(\sqrt{\gamma}t) - (x-1) \cos^2(\sqrt{\gamma}t), \quad (\text{C.3})$$

$$\langle 1 | \rho(t) | 2 \rangle = \langle 2 | \rho(t) | 1 \rangle = -\frac{(\gamma x + x - 1) \sin(2\sqrt{\gamma}t)}{2\sqrt{\gamma}}, \quad (\text{C.4})$$

when prepared similarly in the $\rho(0) = x|g\rangle\langle g| + (1-x)|e\rangle\langle e|$ state. This density matrix is also hermitian at all times, but it is not trace-preserving for all $\gamma \neq 1$.

Now, we couple it to a thermal bath via $\hat{S} = \sigma_x$, and present numerical results in Fig. (C.1). The density matrix is not normalized in that figure as we highlight a few important points: (1) the density matrix in the transient regime may have negative populations. This is in a sense more pathological than being non-trace-preserving, as the latter has a clear physical interpretation, e.g., gain or loss. (2) In spite of this, the coherences are, for the range of parameters swept, complex conjugate of each other. (3) At the transient regime, the system

may accumulate imaginary populations. (4) For certain initial states, the steady-state may even support negative populations. Similar observations are made as we change the coupling matrix from $\hat{S} = \sigma_x$ to $\hat{S} = \sigma_z$ (see Fig. C.2) only that the imaginary populations are now in the order of numerical accuracy. If otherwise not a feature of a hidden physics, this is the most problematic model we study in this work. We briefly discuss a few possible reasons: while we demand a physical preparation for σ , for this model, automatically either of $(\sigma\eta)$ or $(\sigma\eta)^D$ (diagonalized) becomes unphysical. Another possible reason is the additional approximations employed in solving PHRE numerically, e.g., neglecting the imaginary part of the Laplace transform of the bath correlation function (see Ch. 1). In sum, caution must be exercised in applying the PHRE, with particular attention to models having limiting relations between σ , $\sigma\eta$, and $(\sigma\eta)^D$, as the pathologies of the Redfield equation may be amplified [94, 95]. Simulated with the generalized Lindblad equation (GLE), the dynamics for both initial states in Fig. (C.1), is instead stagnant (no change). Further fundamental studies on the theoretical aspects of PHRE are needed. We present the Liouvillian eigenspectrum of this system in the next section, calculated using both PHRE and GLE.

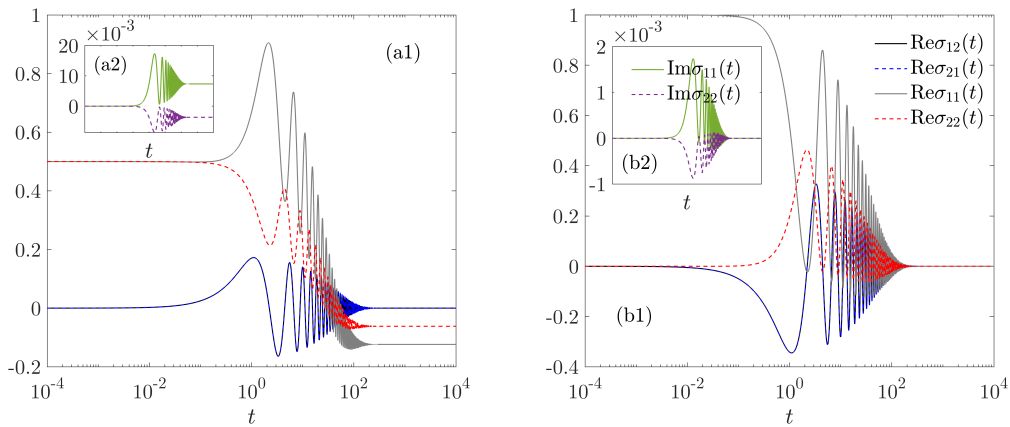
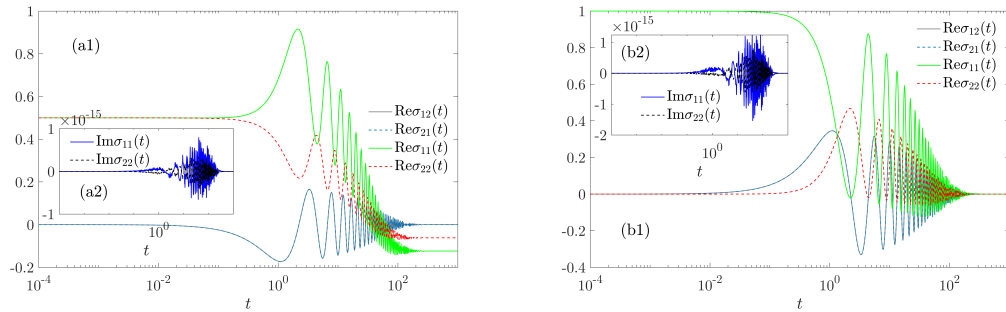
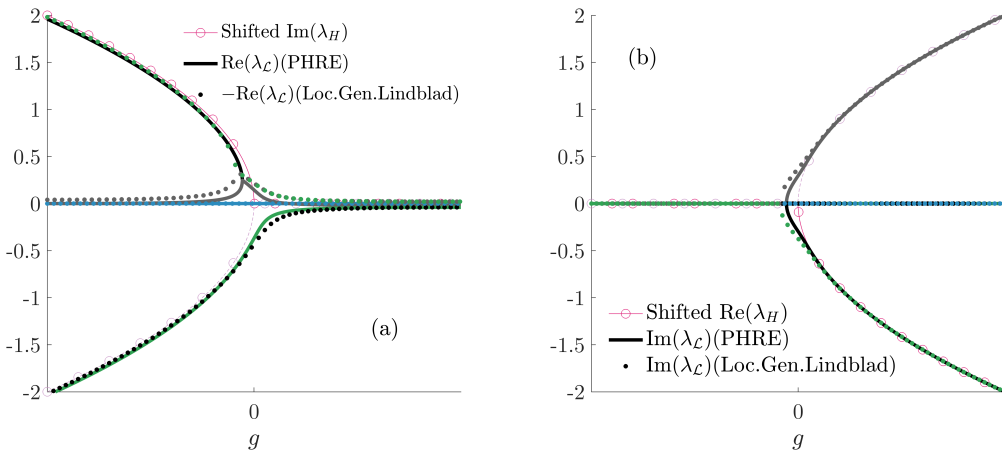


Figure C.1: Numerical simulation using PHRE for the Hamiltonian in Eq. (C.1). In panel (a) we prepare the system with $\sigma(0) = \frac{1}{2}(\mathbf{1} + \sigma_y)$ and in panel (b) we use $\sigma(0) = |g\rangle\langle g|$. Parameters: $\gamma = 0.5$, $T = 4$, $J(\omega) = 0.005\omega$

Exceptional Points

We show here the eigenspectrum of the σ_y -type asymmetric Hamiltonian. Predictions of PHRE agree with those of GLE, although for some unknown reason one is the negative of the other.

Figure C.2: Analog to Fig. (C.1) but $\hat{S} = \sigma_z$.Figure C.3: Real (panel a) and Imaginary (panel b) part of the Liouvillian eigenspectrum of the σ_y -type asymmetric Hamiltonian Eq. (C.1) calculated using PHRE and GLE. Parameters: $a = 0, b = 2, T = 4, J^G(\omega_R, \omega_I) = 0.005\omega_R$.

Bibliography

- [1] C. M. Bender and S. Boettcher, Phys. Rev. Lett. **80**, 5243 (1998), URL <https://link.aps.org/doi/10.1103/PhysRevLett.80.5243>.
- [2] C. M. Bender and P. D. Mannheim, Physics Letters A **374**, 1616 (2010), ISSN 0375-9601, URL <https://www.sciencedirect.com/science/article/pii/S0375960110001933>.
- [3] N. Moiseyev, *Non-Hermitian Quantum Mechanics* (Cambridge University Press, 2011).
- [4] X. Zhu, H. Ramezani, C. Shi, J. Zhu, and X. Zhang, Phys. Rev. X **4**, 031042 (2014), URL <https://link.aps.org/doi/10.1103/PhysRevX.4.031042>.
- [5] R. El-Ganainy, M. Khajavikhan, D. N. Christodoulides, and S. K. Ozdemir, Communications Physics **2**, 37 (2019), URL <https://doi.org/10.1038/s42005-019-0130-z>.
- [6] M.-A. Miri and A. Alù, Science **363**, eaar7709 (2019), <https://www.science.org/doi/pdf/10.1126/science.aar7709>, URL <https://www.science.org/doi/abs/10.1126/science.aar7709>.
- [7] S. K. Özdemir, S. Rotter, F. Nori, and L. Yang, Nature Materials **18**, 783 (2019).
- [8] J. Wiersig, Phys. Rev. A **84**, 063828 (2011), URL <https://link.aps.org/doi/10.1103/PhysRevA.84.063828>.
- [9] J. Kullig, C.-H. Yi, and J. Wiersig, Phys. Rev. A **98**, 023851 (2018), URL <https://link.aps.org/doi/10.1103/PhysRevA.98.023851>.
- [10] H. M. Hurst and B. Flebus, Journal of Applied Physics **132**, 220902 (2022), <https://doi.org/10.1063/5.0124841>, URL <https://doi.org/10.1063/5.0124841>.
- [11] D. R. Nelson and N. M. Shnerb, Phys. Rev. E **58**, 1383 (1998), URL <https://journals.aps.org/pre/pdf/10.1103/PhysRevE.58.1383>.
- [12] R. A. Bertlmann, W. Grimus, and B. C. Hiesmayr, Phys. Rev. A **73**, 054101 (2006), URL <https://link.aps.org/doi/10.1103/PhysRevA.73.054101>.
- [13] F. Benatti and R. Floreanini, Physics Letters B **389**, 100 (1996), ISSN 0370-2693, URL <https://www.sciencedirect.com/science/article/pii/S0370269396012282>.

- [14] A. McDonald, T. Pereg-Barnea, and A. A. Clerk, Phys. Rev. X **8**, 041031 (2018), URL <https://link.aps.org/doi/10.1103/PhysRevX.8.041031>.
- [15] G. L. Celardo and L. Kaplan, Phys. Rev. B **79**, 155108 (2009), URL <https://link.aps.org/doi/10.1103/PhysRevB.79.155108>.
- [16] Y. Ashida, Z. Gong, and M. Ueda, Advances in Physics **69**, 249 (2020), <https://doi.org/10.1080/00018732.2021.1876991>, URL <https://doi.org/10.1080/00018732.2021.1876991>.
- [17] J. Wiersig, Phys. Rev. Res. **4**, 023121 (2022), URL <https://link.aps.org/doi/10.1103/PhysRevResearch.4.023121>.
- [18] J. Li, A. K. Harter, J. Liu, L. de Melo, Y. N. Joglekar, and L. Luo, Nature Communications **10**, 855 (2019), URL <https://doi.org/10.1038/s41467-019-08596-1>.
- [19] W.-C. Wang, Y.-L. Zhou, H.-L. Zhang, J. Zhang, M.-C. Zhang, Y. Xie, C.-W. Wu, T. Chen, B.-Q. Ou, W. Wu, et al., Phys. Rev. A **103**, L020201 (2021), URL <https://link.aps.org/doi/10.1103/PhysRevA.103.L020201>.
- [20] C. Dembowski, H.-D. Gräf, H. L. Harney, A. Heine, W. D. Heiss, H. Rehfeld, and A. Richter, Phys. Rev. Lett. **86**, 787 (2001), URL <https://link.aps.org/doi/10.1103/PhysRevLett.86.787>.
- [21] J. Doppler, A. A. Mailybaev, J. Böhm, U. Kuhl, A. Girschik, F. Libisch, T. J. Milburn, P. Rabl, N. Moiseyev, and S. Rotter, Nature **537**, 76 (2016), URL <https://doi.org/10.1038/nature18605>.
- [22] Z. Lin, Y. Lin, and W. Yi, Phys. Rev. A **106**, 063112 (2022), URL <https://link.aps.org/doi/10.1103/PhysRevA.106.063112>.
- [23] W. Chen, M. Abbasi, B. Ha, S. Erdamar, Y. N. Joglekar, and K. W. Murch, Phys. Rev. Lett. **128**, 110402 (2022), URL <https://link.aps.org/doi/10.1103/PhysRevLett.128.110402>.
- [24] M. Naghiloo, M. Abbasi, Y. N. Joglekar, and K. W. Murch, Nature Physics **15**, 1232 (2019).
- [25] H.-K. Lau and A. A. Clerk, Nature Communications **9**, 4320 (2018), URL <https://doi.org/10.1038/s41467-018-06477-7>.
- [26] S. Khandelwal, N. Brunner, and G. Haack, PRX Quantum **2**, 040346 (2021), URL <https://link.aps.org/doi/10.1103/PRXQuantum.2.040346>.
- [27] J. W. Zhang, J. Q. Zhang, G. Y. Ding, J. C. Li, J. T. Bu, B. Wang, L. L. Yan, S. L. Su, L. Chen, F. Nori, et al., Nature Communications **13**, 6225 (2022), URL <https://doi.org/10.1038/s41467-022-33667-1>.

- [28] Z.-Z. Li, W. Chen, M. Abbasi, K. W. Murch, and K. B. Whaley, *Speeding up entanglement generation by proximity to higher-order exceptional points* (2022), [2210.05048](https://arxiv.org/abs/2210.05048).
- [29] K. Zhang, Z. Yang, and C. Fang, Phys. Rev. Lett. **125**, 126402 (2020), URL <https://link.aps.org/doi/10.1103/PhysRevLett.125.126402>.
- [30] S. Longhi, Phys. Rev. Res. **1**, 023013 (2019), URL <https://link.aps.org/doi/10.1103/PhysRevResearch.1.023013>.
- [31] S. Yao and Z. Wang, Phys. Rev. Lett. **121**, 086803 (2018), URL <https://link.aps.org/doi/10.1103/PhysRevLett.121.086803>.
- [32] D. S. Borgnia, A. J. Kruchkov, and R.-J. Slager, Phys. Rev. Lett. **124**, 056802 (2020), URL <https://link.aps.org/doi/10.1103/PhysRevLett.124.056802>.
- [33] X. Zhang, T. Zhang, M.-H. Lu, and Y.-F. Chen, Advances in Physics: X **7**, 2109431 (2022), <https://doi.org/10.1080/23746149.2022.2109431>, URL <https://doi.org/10.1080/23746149.2022.2109431>.
- [34] Z. Lin, H. Ramezani, T. Eichelkraut, T. Kottos, H. Cao, and D. N. Christodoulides, Phys. Rev. Lett. **106**, 213901 (2011), URL <https://link.aps.org/doi/10.1103/PhysRevLett.106.213901>.
- [35] A. Regensburger, C. Bersch, M.-A. Miri, G. Onishchukov, D. N. Christodoulides, and U. Peschel, Nature **488**, 167 (2012), URL <https://doi.org/10.1038/nature11298>.
- [36] I. I. Arkhipov, A. Miranowicz, F. Minganti, and F. Nori, Phys. Rev. A **102**, 033715 (2020), URL <https://link.aps.org/doi/10.1103/PhysRevA.102.033715>.
- [37] W. Chen, M. Abbasi, Y. N. Joglekar, and K. W. Murch, Phys. Rev. Lett. **127**, 140504 (2021), URL <https://link.aps.org/doi/10.1103/PhysRevLett.127.140504>.
- [38] F. Minganti, A. Miranowicz, R. W. Chhajlany, and F. Nori, Phys. Rev. A **100**, 062131 (2019), URL <https://link.aps.org/doi/10.1103/PhysRevA.100.062131>.
- [39] Q. Du, K. Cao, and S.-P. Kou, Phys. Rev. A **106**, 032206 (2022), URL <https://link.aps.org/doi/10.1103/PhysRevA.106.032206>.
- [40] T. Ohlsson and S. Zhou, Phys. Rev. A **103**, 022218 (2021), URL <https://link.aps.org/doi/10.1103/PhysRevA.103.022218>.
- [41] K. Cao and S.-P. Kou, *Statistical mechanics for non-hermitian quantum systems* (2023), [2304.04691](https://arxiv.org/abs/2304.04691).
- [42] G. Scolarici and L. Solombrino, Czechoslovak Journal of Physics **56**, 935 (2006), URL <https://doi.org/10.1007/s10582-006-0389-7>.

- [43] C. F. de Morisson Faria and A. Fring, Journal of Physics A: Mathematical and General **39**, 9269 (2006), URL <https://dx.doi.org/10.1088/0305-4470/39/29/018>.
- [44] A. Mostafazadeh, Journal of Mathematical Physics **43**, 205 (2002), ISSN 0022-2488, https://pubs.aip.org/aip/jmp/article-pdf/43/1/205/7481018/205_1_online.pdf, URL <https://doi.org/10.1063/1.1418246>.
- [45] D. A. Lidar, *Lecture notes on the theory of open quantum systems* (2020), [1902.00967](https://arxiv.org/abs/1902.00967).
- [46] H.-P. Breuer and F. Petruccione, *The Theory of Open Quantum Systems* (Oxford University Press, 2007), ISBN 0199213909.
- [47] A. Nitzan, *Chemical Dynamics in Condensed Phases: Relaxation, Transfer, and Reactions in Condensed Molecular Systems* (New York: Oxford University Press, 2006).
- [48] G. G. Pyrialakos, H. Ren, P. S. Jung, M. Khajavikhan, and D. N. Christodoulides, Phys. Rev. Lett. **128**, 213901 (2022), URL <https://link.aps.org/doi/10.1103/PhysRevLett.128.213901>.
- [49] G. Cipolloni and J. Kudler-Flam, *Non-hermitian hamiltonians violate the eigenstate thermalization hypothesis* (2023), URL <https://arxiv.org/abs/2303.03448>.
- [50] B. Jaramillo Ávila, C. Ventura-Velázquez, R. d. J. León-Montiel, Y. N. Joglekar, and B. M. Rodríguez-Lara, Scientific Reports **10**, 1761 (2020), URL <https://doi.org/10.1038/s41598-020-58582-7>.
- [51] Z. Ahmed, Journal of Physics A: Mathematical and General **36**, 10325 (2003), URL <https://dx.doi.org/10.1088/0305-4470/36/41/005>.
- [52] A. MOSTAFAZADEH, International Journal of Geometric Methods in Modern Physics **07**, 1191 (2010), URL <https://doi.org/10.1142%2Fs0219887810004816>.
- [53] B. Gardas, S. Deffner, and A. Saxena, Scientific Reports **6**, 23408 (2016), URL <https://doi.org/10.1038/srep23408>.
- [54] C. Jarzynski, Phys. Rev. Lett. **78**, 2690 (1997), URL <https://link.aps.org/doi/10.1103/PhysRevLett.78.2690>.
- [55] M. Kilgour and D. Segal, Phys. Rev. E **98**, 012117 (2018), URL <https://link.aps.org/doi/10.1103/PhysRevE.98.012117>.
- [56] F. Ivander, N. Anto-Sztrikacs, and D. Segal, New Journal of Physics **24**, 103010 (2022), URL <https://dx.doi.org/10.1088/1367-2630/ac9498>.
- [57] T. J. YAHYA, *Steady-state transport properties of anharmonic systems* (2013).

- [58] J. Julve, R. Cepedello, and F. J. de Urries, *The complex dirac delta, plemelj formula, and integral representations* (2016), [1603.05530](https://arxiv.org/abs/1603.05530).
- [59] I. Pallikara, P. Kayastha, J. M. Skelton, and L. D. Whalley, Electronic Structure **4**, 033002 (2022), URL <https://dx.doi.org/10.1088/2516-1075/ac78b3>.
- [60] M. J. Blacker and D. L. Tilbrook, Phys. Rev. A **104**, 032211 (2021), URL <https://link.aps.org/doi/10.1103/PhysRevA.104.032211>.
- [61] F. Bagarello, Theoretical and Mathematical Physics **171**, 497 (2012).
- [62] T. G. Philbin, New Journal of Physics **14**, 083043 (2012), URL <https://dx.doi.org/10.1088/1367-2630/14/8/083043>.
- [63] P. Lewalle and K. B. Whaley, Phys. Rev. A **107**, 022216 (2023), URL <https://link.aps.org/doi/10.1103/PhysRevA.107.022216>.
- [64] H. Eleuch and I. Rotter, Phys. Rev. A **95**, 022117 (2017), URL <https://link.aps.org/doi/10.1103/PhysRevA.95.022117>.
- [65] I. Rotter, *The role of exceptional points in quantum systems* (2010), [1011.0645](https://arxiv.org/abs/1011.0645).
- [66] A. Das, Journal of Physics: Conference Series **287**, 012002 (2011), URL <https://dx.doi.org/10.1088/1742-6596/287/1/012002>.
- [67] Q. Zhong, J. Ren, M. Khajavikhan, D. N. Christodoulides, i. m. c. K. Özdemir, and R. El-Ganainy, Phys. Rev. Lett. **122**, 153902 (2019), URL <https://link.aps.org/doi/10.1103/PhysRevLett.122.153902>.
- [68] B. Peng, Şahin Kaya Özdemir, M. Liertzer, W. Chen, J. Kramer, H. Yilmaz, J. Wiersig, S. Rotter, and L. Yang, Proceedings of the National Academy of Sciences **113**, 6845 (2016), <https://www.pnas.org/doi/pdf/10.1073/pnas.1603318113>, URL <https://www.pnas.org/doi/abs/10.1073/pnas.1603318113>.
- [69] S. Dogra, A. A. Melnikov, and G. S. Paraoanu, Communications Physics **4**, 26 (2021), URL <https://doi.org/10.1038/s42005-021-00534-2>.
- [70] D. Yu and F. Vollmer, Communications Physics **4**, 77 (2021), URL <https://doi.org/10.1038/s42005-021-00575-7>.
- [71] Y.-L. Fang, J.-L. Zhao, Y. Zhang, D.-X. Chen, Q.-C. Wu, Y.-H. Zhou, C.-P. Yang, and F. Nori, Communications Physics **4**, 223 (2021).
- [72] I. I. Arkhipov, A. Miranowicz, O. Di Stefano, R. Stassi, S. Savasta, F. Nori, and i. m. c. K. Özdemir, Phys. Rev. A **99**, 053806 (2019), URL <https://link.aps.org/doi/10.1103/PhysRevA.99.053806>.

- [73] W. D. Heiss, M. Müller, and I. Rotter, Phys. Rev. E **58**, 2894 (1998), URL <https://link.aps.org/doi/10.1103/PhysRevE.58.2894>.
- [74] G.-Q. Zhang, Z. Chen, D. Xu, N. Shammah, M. Liao, T.-F. Li, L. Tong, S.-Y. Zhu, F. Nori, and J. Q. You, PRX Quantum **2**, 020307 (2021), URL <https://link.aps.org/doi/10.1103/PRXQuantum.2.020307>.
- [75] K. Takata, N. Roberts, A. Shinya, and M. Notomi, Phys. Rev. A **105**, 013523 (2022), URL <https://link.aps.org/doi/10.1103/PhysRevA.105.013523>.
- [76] H. Benisty, C. Yan, A. Degiron, and A. Lupu, Journal of Lightwave Technology **30**, 2675 (2012).
- [77] U. Weiss, *Quantum Dissipative Systems* (Singapore:World Scientific, 1999).
- [78] H. Ramezani, D. N. Christodoulides, V. Kovanis, I. Vitebskiy, and T. Kottos, Phys. Rev. Lett. **109**, 033902 (2012), URL <https://link.aps.org/doi/10.1103/PhysRevLett.109.033902>.
- [79] J. Um, K. E. Dorfman, and H. Park, Phys. Rev. Res. **4**, L032034 (2022), URL <https://link.aps.org/doi/10.1103/PhysRevResearch.4.L032034>.
- [80] F. Ivander, N. Anto-Sztrikacs, and D. Segal, *Hyper-acceleration of quantum thermalization dynamics by bypassing long-lived coherences: An analytical treatment* (2023), [2301.06135](https://arxiv.org/abs/2301.06135).
- [81] Y. N. Joglekar and A. K. Harter, Photon. Res. **6**, A51 (2018), URL <https://opg.optica.org/prj/abstract.cfm?URI=prj-6-8-A51>.
- [82] M. Ueda, Nature Reviews Physics **2**, 669 (2020), URL <https://doi.org/10.1038/s42254-020-0237-x>.
- [83] K. Mallayya, M. Rigol, and W. De Roeck, Phys. Rev. X **9**, 021027 (2019), URL <https://link.aps.org/doi/10.1103/PhysRevX.9.021027>.
- [84] D. Xu and J. Cao, Frontiers of Physics **11**, 110308 (2016).
- [85] J. H. Fetherolf, D. Golež, and T. C. Berkelbach, Phys. Rev. X **10**, 021062 (2020), URL <https://link.aps.org/doi/10.1103/PhysRevX.10.021062>.
- [86] N. Anto-Sztrikacs, F. Ivander, and D. Segal, The Journal of Chemical Physics **156**, 214107 (2022), ISSN 0021-9606, https://pubs.aip.org/aip/jcp/article-pdf/doi/10.1063/5.0091133/16543355/214107_1_online.pdf, URL <https://doi.org/10.1063/5.0091133>.
- [87] N. Anto-Sztrikacs, A. Nazir, and D. Segal, PRX Quantum **4**, 020307 (2023), URL <https://link.aps.org/doi/10.1103/PRXQuantum.4.020307>.

- [88] F. Ivander, N. Anto-Sztrikacs, and D. Segal, Phys. Rev. E **105**, 034112 (2022), URL <https://link.aps.org/doi/10.1103/PhysRevE.105.034112>.
- [89] T. Becker, A. Schnell, and J. Thingna, Phys. Rev. Lett. **129**, 200403 (2022), URL <https://link.aps.org/doi/10.1103/PhysRevLett.129.200403>.
- [90] Y.-L. Zhou, X.-D. Yu, C.-W. Wu, X.-Q. Li, J. Zhang, W. Li, and P.-X. Chen, *Accelerating relaxation through liouvillian exceptional point* (2023), [2305.12745](https://arxiv.org/abs/2305.12745).
- [91] D. Manzano, AIP Advances **10**, 025106 (2020), <https://doi.org/10.1063/1.5115323>, URL <https://doi.org/10.1063/1.5115323>.
- [92] K. G. Zloshchastiev and A. Sergi, Journal of Modern Optics **61**, 1298 (2014), <https://doi.org/10.1080/09500340.2014.930528>, URL <https://doi.org/10.1080/09500340.2014.930528>.
- [93] S. S. Mukherjee and P. Roy, *On pseudo-hermitian hamiltonians* (2014), [1401.5255](https://arxiv.org/abs/1401.5255).
- [94] Y. C. Cheng and R. J. Silbey, The Journal of Physical Chemistry B **109**, 21399 (2005), URL <https://doi.org/10.1021/jp051303o>.
- [95] A. Ishizaki and G. R. Fleming, The Journal of Chemical Physics **130** (2009), ISSN 0021-9606, 234110, https://pubs.aip.org/aip/jcp/article-pdf/doi/10.1063/1.3155214/13131389/234110_1_online.pdf, URL <https://doi.org/10.1063/1.3155214>.